The University of Nottingham
School of Pharmacy

# MEASUREMENT AND CHARACTERISATION OF GLYCANS ON SURFACES

**Thesis submitted to the University of Nottingham**
**for the degree of Masters of Research**

**ADEOLU OLUWASANMI, BSc.**

**JULY 2013**

**University of Nottingham**

**Contents**

**ABBREVIATIONS**

AFM: Atomic Force Microscopy

XPS: X-ray Photoelectron Spectroscopy

ToF-SIMS: Time of Flight – Secondary Ion Mass Spectrometry

HPLC: High Performance Liquid Chromatography

PBS: Phosphate Buffered Saline

EMCS: 6-maleimidohexanoic acid N-hydroxysuccinimide ester (its main synonym as shown on Sigma Aldrich's chemical catalogue)

# Abstract

Glycans are a diverse group of compounds, which include glycoproteins and glycolipids and are ubiquitously present on cell surfaces. As a result glycan interactions are responsible for a number of medical conditions such as autoimmune diseases like rheumatoid arthritis, viral infections and as a cause of inflammation. Fully understanding the structure and function of these compounds requires the use of innovative surface analytical methods for screening large numbers of different glycans against serums, for biomarkers attributed to these illnesses. The main objective of this work was to produce and characterise glycan surfaces with reliable, reproducible and quantitative readouts. However, the complex nature of glycans means that analysis of their interactions on microarray surfaces doesn't always produce reliable readouts. The surfaces analysed also include commercially available amine coated slides for quality assurance and maleimide slides, which were produced by treating amine coated slides with 6-maleimidohexanoic acid N-hydroxysuccinimide ester ('EMCS' as denoted by Sigma Aldrich). Thiolated sugars can then react and covalently bond with the maleimide surfaces. Heterogeneous glycan immobilisation within spots is characterised using surface chemical analysis and compared to literature observation. The progress of the project titled "Measurement and Characterisation of Glycans on Surfaces" to date involved producing microarrays of β-D-thioglucose on a maleimide functionalised surface in order to see how phosphate buffered saline affected the surface chemistry and characterisation of the spots on the surface by using time of flight – secondary ion mass spectrometry.

# 1. Introduction

The aim of this project is to produce glycan surfaces and characterise them in order to discover the cause of heterogeneous sugar distributions such that better quality arrays can be produced in future to support the expanding area of glycomics.

Surface interactions of glycans are ubiquitously found throughout the human body, e.g. glycolipids which serve as markers for cellular recognition, and on the protein envelope of viruses which are used to infect native cells[1]. These interactions can be mimicked artificially by producing surfaces containing these glycan compounds and screening them for interactions with various substrates such as cell surface receptors and foreign antigens. Surface chemical characterisation is the study of the characteristics and interactions present at the interface between two or more distinct phases such as glycan spots on a microarray[2]. There has been more focus on the physiochemical characterisation of these surfaces where only the surface chemistry and the physical interactions on the solid surfaces are considered without the biological implications. The understanding of organic molecules such as carbohydrates with solid surfaces like glass slides is still limited[2] and will be covered throughout this project. In time the biological and clinical potential of this research will be determined. This may include producing models for the surface glycan ligands cells and screening them against various biomarkers which are indicative of many illnesses[3].

Surfaces which are often used in surface chemistry analysis are glass slides, microbeads and silicon plates[4]. These surfaces are often pre-treated to ensure optimal or minimal interaction between the surface and the substance in question. One example of a glass slide being pre-treated would be the production of maleimide coated glass slides from amine coated slides[5]. The maleimide groups on the surface can then covalently bond with thiol groups present on thiolated sugars. This is made possible by the use of established linker chemistry allowing for covalent bonding of the thiolated sugars with the surface.

A microarray is a miniaturised high-throughput slide used in the analysis and testing of the activities of a large number of biological materials simultaneously[5]. They are commonly used in the field of glycomics, which is the study of biological glycans where each glycan's structure, function and interactions are studied. Microarrays are the best format for screening and discovering carbohydrate's biological function in a high-throughput fashion [5-7]. An issue with microarray use is the uniformity of the analyte within each spot, which is affected by many factors including printing methods by the operator and the presence of salt ions and other substances (contaminants), which can affect the spot shape, size and distribution of compounds within each spot. The effect of these factors will be addressed in this report. Microarrays are typically produced on glass slides because microarray printers have been designed to accommodate their size and shape. A time of flight – secondary ion mass spectrometer has a sample holder called a stage. The stage is fixed and holds the sample holder

which is designed to hold glass slides. This means surface preparation/treatment, printing and then analysis of the slides are done on the same slide by making all equipment and techniques compatible with glass slides. By using an in-built microscope, the operator can input various x,y, coordinates that are attributed to each spot or a group of spots. This allows the scanning of numerous samples on one slide without having to analyse the entire surface which saves time and resources. The microarray slides are also easy to store in slide mailers which makes them very convenient for use.

Another type of surface which can be used to characterise the interactions of glycans are microbeads. Microbeads can be used for analysing live whole cell surface interactions in suspensions. The glycans involved could be glycoproteins which are found on cell surfaces. These cells would perish in the vacuum conditions present during certain surface analysis techniques such as ToF-SIMS. Microbeads differ from glass slides in their uses in surface chemistry[4]. A glass slide can be functionalised specifically for a particular substrate type to produce microarrays for quantitative research, such as a maleimide functionalised glass slide to analyse it's interaction with thiolated glycans. Microbeads possess a larger surface-area to volume ratio than glass slide because their surfaces are curved due to their spherical shape. However this makes simultaneous analysis of specific regions of each microbead difficult[8]. The entire surface of a glass slide and all of the spots on a microarray can be analysed on the same analysis run because all of the spots are at the same angle from the analyser (on a flat surface). Multiple glycans can be printed on the same surface and be

distinguished from each other. Microbeads cannot be made into microarrays due to their spherical shape which prevents complete surface analysis and the great difficulty in handling individual microbeads[4, 9]. Microbead sizes range from 0.5 to 500μm in diameter. Even if a single layer of immobilized microbeads were attached to a flat surface, the glycan layer would be present at different depths. AFM could be used to analyse these surfaces but other techniques like ToF-SIMS would be unable to detect ions from deeper depths due to its limited detection range of 2 nm. These factors show us that microbeads are not a suitable surface to characterise glycans in this particular research.

Another possible surface type to analyse the surface interaction of glycans are silicon plates. We seldom see them used as solid surfaces for microarrays because they are more expensive than glass slides and do not always come in the same size as a typical 25mm by 75mm as glass slides come in. Several techniques which will be described later on including, maleimide coating commercially acquired amine coated slides inside Coplin jars, producing microarrays using an inkjet microarrayer and carrying out fluorescence spectroscopy on fluorescamine assayed slides were possible or easier to accomplish because the glass slides used were 25mm by 75mm in size. If smaller slides were needed then the existing glass slides could have been cut to size with a diamond cutter pen. All of these techniques and more are usually present to a slide of 25mm by 75mm. Silicon plates are conductive making them ideal for insulated surfaces like a glycan array. Aluminium foil was used to increase surface conductivity coupled with charge compensation to ensure an even distribution of charge on

the surface during analysis. So after reviewing three types of surfaces used in surface chemistry, functionalised microscope glass slides provide the best format for producing carbohydrate microarrays in this project which is why they are used.

There are many research groups that carry out research in surface chemistry involving the use of carbohydrate microarrays. These groups have their own methods for carrying their research and making a contribution to carbohydrate surface chemistry. It is unlikely for multiple scientific groups to carry out the exact same research unless a degree of collaboration is established. Normally some scientific groups will focus on the development of techniques pertinent to the field (such as solid phase synthesis of carbohydrates) while others use existing techniques to characterise new surface interactions and chemistries[1]. Glycans are one of the most prevalent biomolecules present in nature[1, 10]. They are frequent targets for microbes and toxins and are part of membrane recognition sites making them their research important for clinical science. Synthesis of glycans makes up a large amount of the current research in sugar chemistry today. The next chapters will discuss two different routes for acquiring glycans in order to carry out glycan research which could include microarray analysis.

Acquiring thiolated oligosaccharides for this current project is difficult for many reasons. Some of these reasons include, that some of these oligosaccharides are not found naturally at a high enough amount to be extracted and purified cost effectively from biological sources[11]. Therefore

they will have to be synthesized. However the synthesis of oligosaccharides can involve a large amount of steps and a long time while still requiring a great deal of expertise. Therefore many commercial chemical suppliers do not produce these oligosaccharides and the ones that do tend to produce by order which leads to very expensive orders. As a result different scientific groups acquire their sugars using the methods they are most comfortable with whether it's by synthesis, extraction-purification or by purchasing them.

Peter Seeberger is known for his method of synthesizing oligosaccharides using solid phase synthesis of carbohydrates[1].

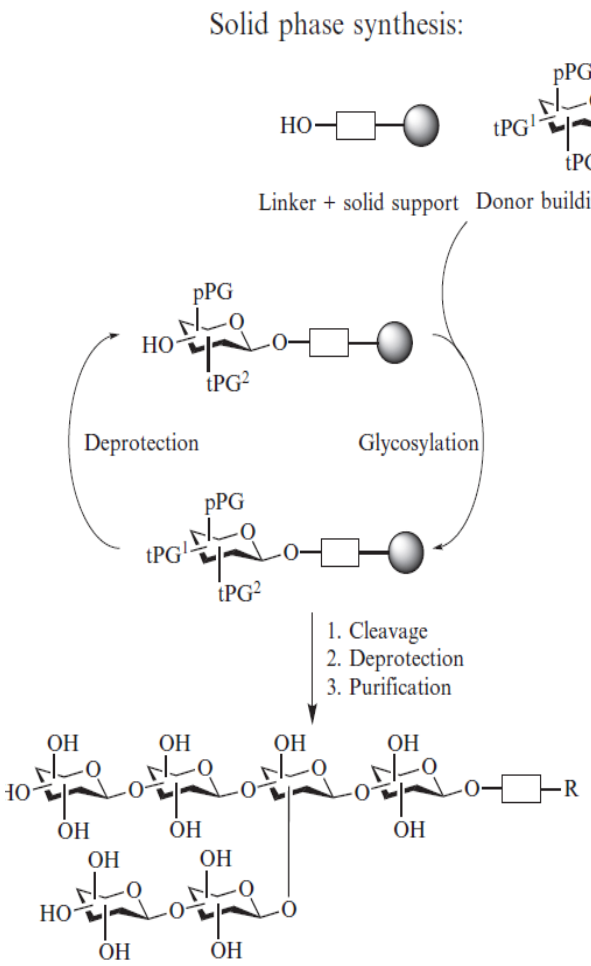


The method of solid phase synthesis:

First a hydroxyl linker which is bound to a solid support, is used to substitute a leaving group on the donor building block structure.

This step shows the deprotection and glycosylation cycle where the current terminal sugar compound contains a temporary protection group. After deprotection of this group the hydroxyl group is vulnerable to condensation reactions with the next donor building block[1].

If branching is required, then secondary temporary groups are used on side hydroxyl groups. These groups are deprotected to enable branching at the correct stereocentre.

Figure 1 – solid phase synthesis of oligosaccharides diagram[1].

Sonication has already been shown to improve the glycosylation steps in solution phase synthesis of oligosaccharides and Tanifum (2010) successfully incorporated the method of sonication to the already established solid phase synthesis method to improve the glycosylation time and yield[10].

Terminal sugar monomer units possess four hydroxyl groups capable of forming glycosidic bonds with other sugar monomers. That is four stereocentres that will have to be controlled at each

reaction step. Solid phase synthesis of peptides for example is much easier due to the linearity of peptide formation to form long chain polypeptides which only fold at specific R group interactions along the chain. This is what makes the synthesis of oligosaccharides difficult and time consuming with a high degree of expertise needed to ensure a good yield.

Dell et al. is known for isolating carbohydrates from natural sources like living tissues and cell cultures[12] and purifies the sugars for use. This can be a slow and tedious method which leads to poor yields. However some of these sugars are currently unavailable from artificial synthesis, which means extraction from natural sources is the only currently available method. The reason for this is due to carbohydrates ability to form highly specific branched polymers which are readily produced in biological systems but are difficult to produce artificially with current techniques. After successful extraction these sugars may have to undergo sample preparation to make them suitable for surface analysis, such as attaching a thiol linker for maleimide functionalised glass slides.

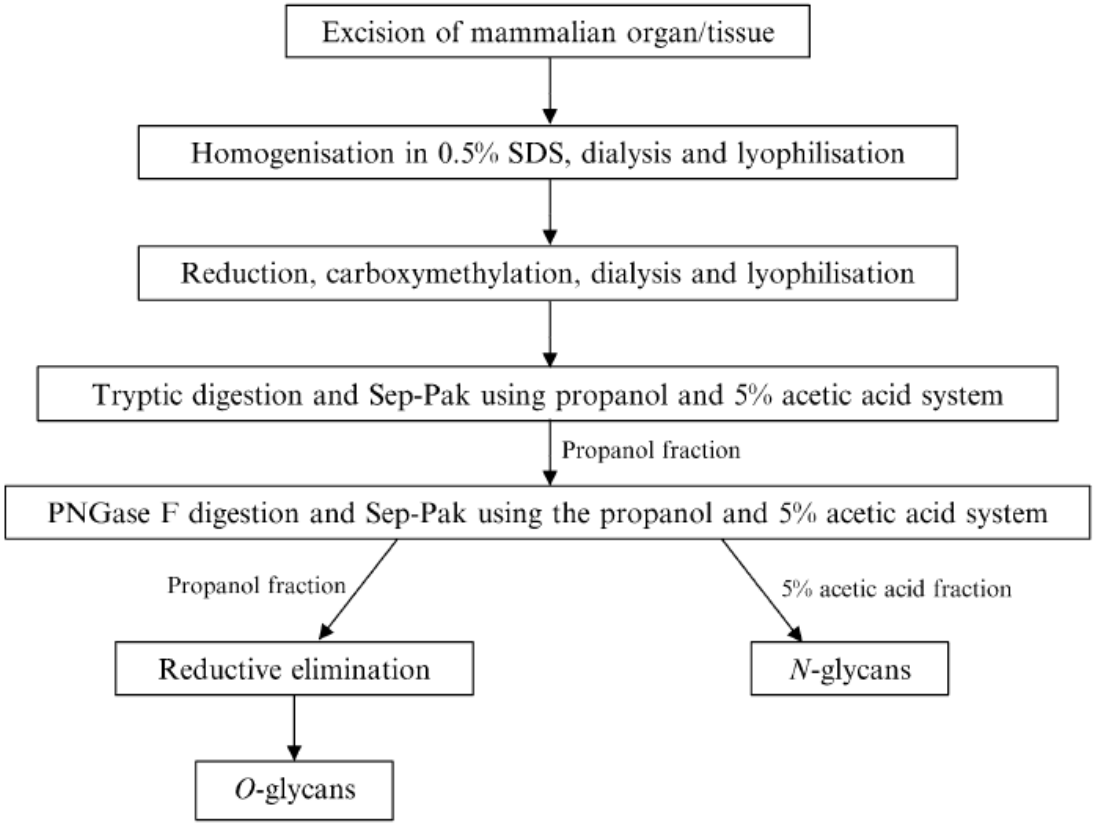


Figure 2 - Overview of the extraction steps for acquiring glycans from biological sources such as cells, organs and tissues[12].

Both of these methods have a lot of steps and require a great deal of care and expertise to carry out. This is why each group opts for the method that best suits them due to their experience and the form of the biological question that their approach is tailored to answer.

# 2. Literature Review - Overview

## 2.1 Background

The field of glycomics has only begun to gain momentum in research progress, in more recent years compared to its other 'omic' counterparts such as genomics and proteomics which have been in the spotlight longer[7, 13]. An omic field is a particular research topic focused on the structure, function and mapping of the components in question across all biological environments either in a particular organism (i.e. the human genome project) or across all organisms and even artificially created ones[7, 13]. Therefore all omic fields require a great deal of effort and collaboration for successful progress and eventual completion. This project titled *"Measurement and Characterisation of Glycans on Surfaces."* firstly involves the production of carbohydrate microarrays and then the analysis of glycans on such arrays using various techniques to gain knowledge as to the identity of the species within the structure and their distribution throughout each spot. The techniques utilized for microarray analysis include ToF-SIMS, AFM and XPS with possible other techniques being explored as the project continues.

## 2.2 Use of Microarrays

As discussed in the introduction, a microarray is a miniaturised high-throughput slide used in the analysis and testing of the activities of large numbers of biological materials simultaneously[5]. A bio array is an arrangement of biological material such as glycans proteins and DNA, which is organised and repeating (i.e. rows and columns)[5, 14-17]. Glycans are ubiquitously present throughout the body. More than half of polypeptides present are covalently modified by glycans alone[18] where they are present covalently bonded to proteins and lipids. Post translational modifications (PTMs) are the modifications that occur after a protein is formed after its translation. As a result of these PTMs it is believed that more than half of all proteins are glycoproteins[19]. In glycoprotein linkages there are on average 13 different monosaccharides involved per linkage and above 40 linkages connecting the glycan to the protein where each one has a different structure and function. When you take into account that these linkages also include oligosaccharides and complex branched saccharides you soon see the exponential variation in structure and function of glycans in the body[18]. The use of microarrays allows for a rapid simultaneous analysis of biomolecule interactions in a single assay. Potentially thousands of structurally different glycans can be placed on a single microarray slide and analysed simultaneously[13]. For example, if someone were to use ToF-SIMS to analyse such a surface, at a resolution of 256µm by 256µm it would take around 385minutes to screen 1000 different glycans using ToF-SIMS. The amount of glycan material required is very

small which is beneficial because many of them are typically difficult to synthesize/extract or too expensive to purchase in large quantities (above 1g) for many research group budgets[5]. A quote from Carbosynth™ estimated the synthesis of this mannose sugar at £2500 for 10mg.

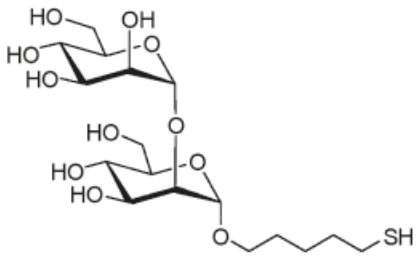


Man(α1-2)Manα

Figure 3 – Structure of a mannose disaccharide with a thiol terminated linker[5].

Because of all these reasons, microarrays are an integral part of many surface analysis work such as those carried out in this report and are the main subject of this project from the initial stages and throughout the entire project due to their through-put, easy storage, speed and cost effectiveness of analysis.

## 2.3 Analytical Techniques Available

In this project, work was carried done with surfaces which were pre-treated (i.e. amine coated surfaces) and then a known or unknown compound arrayed onto its surface. The end result is a dry surface with covalent interaction between the glycan and the surface itself. As a result it's best to use techniques that do not drastically alter the already present conditions on the surface. Solid state NMR could have been used if not for the fact that the high amount of hydrogen environments present within sugars including the numerous hydroxyl groups, which have led to NMR spectra that contained too much information and a large broad peak for hydroxyl groups which would cover many peaks. Although the NMR spectra would identify aspects of a carbohydrate it would be difficult to discern how many monomers were present and their types[20]. Atomic absorption spectroscopy involves actually igniting the sample and analysing the detected ions. This means that the surface would have to be destroyed which removes the concept of a repeatable useable microarray surface. This left us with techniques that minimize sample destruction and maintain the solid surface while only affecting the very top region of the surface. Several techniques fit these criteria well including ToF-SIMS, AFM, XPS, IR, UV-Vis, fluorescence spectroscopy and raman spectroscopy. I was particularly interested in incorporating microscopy into this project in order to produce images of the surfaces. While AFM does provide a clear image of the surface, chemical analysis couldn't be carried out

simultaneously to imaging procedures unless AFM was coupled with another technique such as IR spectroscopy (AFM-IR)[21].

### 2.4 Current Progress of Glycan Immobilisation on Microarrays Research

A paper titled *Surface Characterisation of Carbohydrate Microarrays* by Scurr et al contains aspects that are very similar to the scope of this project[5]. In total they used 17 different saccharides with a PBS control. The saccharides all had linker arms terminated with a thiol group that would covalently bond with the maleimide groups on the slide surface after spotting[5]. The maleimide groups on the surface were present due to a previous reaction of 6-maleimidohexanoic acid N-hydroxysuccinimide ester (EMCS) with a commercially acquired amine coated glass slides from Sigma Aldrich. The authors understood that while carbohydrate microarrays were essential as diagnostic tools for determining the function and characteristics of glycans they were lacking in spot uniformity throughout the array. Spots were not reproducible and there was an uneven distribution of compounds. Spot size changed depending on the concentration of the saccharide in which the more concentrated the spot the larger its diameter. This was due the saccharides decreasing the surface tension of their solution leading to large sessile drops. Phosphate buffered saline (PBS) is a buffer solution containing sodium chloride, sodium phosphate and potassium chloride and other ionic compounds[22]. It is used to maintain a constant pH and it's commonly used in sugar chemistry and many other facets of biological research. The use of PBS which they stated *"is employed in virtually*

*all biological protocols, may also hinder microarray analysis"*[5]. The use of PBS in this work led to the deposition of salt ions such as NaCl at the centre of the spots. These regions were removable after rinsing but it left a ring pattern instead of a solid spot which contained no indication of saccharide immobilisation to the surface[5]. However this did not occur for all of the saccharides used and the reasons for this will also be investigated in future work. The presence of deposited PBS hinders some of the saccharide reaction with the surface. This is not ideal because it means there is an entire region of analyte missing. The proposed reason for why this ring phenomenon occurs is due to the way the spot dries and the different solubility's of the solutes within the drops[5]. As soon as the drop is placed on the surface it begins to evaporate in the right environmental conditions such as air pressure, temperature which affects the kinetic energy of the solvent molecules and humidity if the solvent concerned is water.[22] . Different solutes have different solubilities and those that are less soluble will become saturated sooner as the spot dries. The saturated solutes then precipitate out of solution. In the case of Scurr et al, the unreacted thiolated saccharides precipitated first nearer the spot edges[5]. Eventually the spot completely evaporates and the most soluble solutes which will be the components of PBS, will precipitate last at the centre of the spot hindering carbohydrate reactions[5]. Because the use of PBS is employed in most biological protocols[5] including microarray analysis it will be worth studying its effects on the carbohydrate microarrays that were produced.

# 3. Methods

## 3.1 Time of Flight – Secondary Ion Mass Spectrometry

A technique that only analyses the surface of a material is time of flight – secondary ion mass spectrometry (ToF-SIMS). Analysis of the surface involves firing primary ions from an ion source onto the sample surface. Examples of primary ions used include $Bi_n^+$ and $C_{60}^+$.

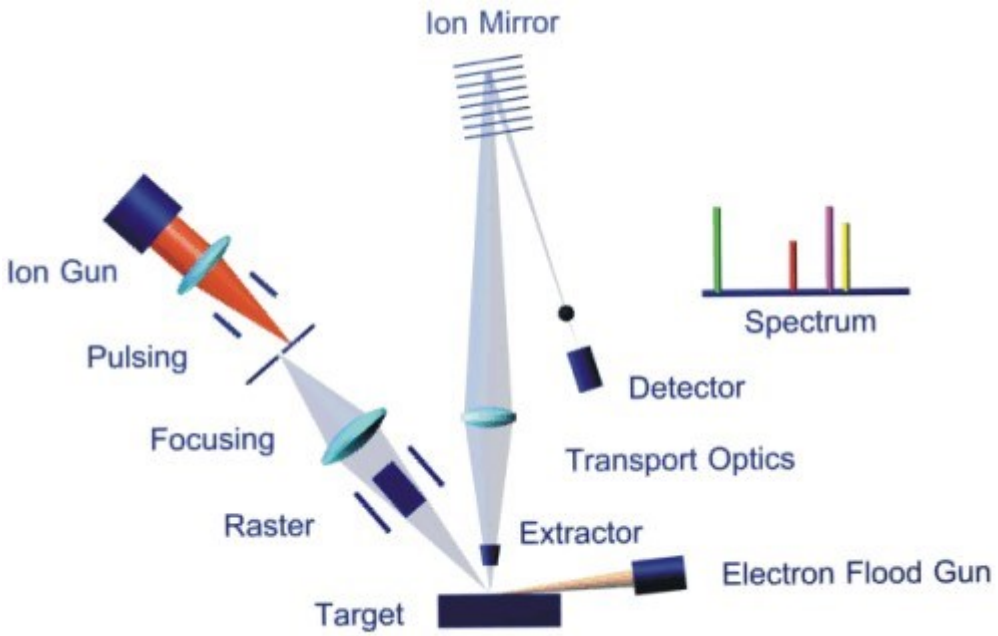


Figure 4 – Diagram depicting the mechanical operation of ToF-SIMS analysis[18].

The ions collide with the surface at high speeds providing the energy required to break covalent bonds on the sample[23]. As a result ToF-SIMS is regarded as a destructive analytical technique. The energy from the collision allows secondary ions from the sample to be emitted from the surface. These secondary ions are accelerated by a fixed potential which balances the kinetic

energy of the ions equally[23]. As a result all of the secondary ions have the same kinetic energy. The only difference between them is their mass. Heavier ions will travel slower than lighter ones and are detected later on. Therefore the "Time of Flight" of each ion is directly related to its mass[23]. Once an ion is detected the detector becomes insensitive for a period of time (~40 nanoseconds) before becoming sensitive to the arrival of new ions. This is called dead time and it may not be an issue if the arrival of ions of all masses was linear in number throughout the detection phase. However high intensity mass fragments will be detected with a degree of uncertainty especially if their intensities fluctuate significantly below 200 nanoseconds[24]. Another great advantage of ToF-SIMS is the ability to generate pixel images of the scan area where higher intense regions of the sample can be clearly distinguished from lower intense regions from the point of view of specific ions[5, 23]. The distribution of ions on the sample scan area can be clearly seen. Like in XPS, the sample analysed by ToF-SIMS must be carried out in vacuum conditions, typically at a pressure of $2 \times 10^{-6}$ mbar[23]. This is to stop primary and secondary ions from colliding with atmospheric atoms and compounds. The emission of primary ions is a form of alpha radiation and alpha radiation has low penetration through air when compared to beta/gamma radiation. Therefore it is very important that ToF-SIMS takes place within ultrahigh vacuum conditions. Wet samples cannot be analysed by ToF-SIMS because even after vacuuming is completed the liquid would evaporate within the analysis chamber and form a gas. Water present at the surface would hinder charge also compensation which would lead to incorrect ion distributions due to certain regions of the surface being more or less readily

ionisable[25]. The majority of liquid substances would vaporize much faster under such low atmospheric pressures which are seen on the phase diagrams of many substances. There are many ion beam sources available for ToF-SIMS use. The ion source currently used in this project is the $Bi^+$ source. It is a heavy metal ion source which is required to yield higher mass secondary ions from the sample surface. This is an attractive ability to utilize for the analysis of organic and bio-organic substances such as glycans. Other ion sources such as $Cs^+$ and $C_{60}^+$ can also be used to perform a technique called depth profiling.

Because ToF-SIMS involves the removal of ions from the samples surface it can be described as a destructive technique. This can be a useful trait because it allows a deeper analysis of the surface to be carried out. This technique is called depth profiling and it involves focusing the ion beam at the sample area. The ion beam erodes away at the surface and analysis of ions at different depths can be carried out. This is useful for showing how the chemical composition of the surface changes as you probe deeper. The thickness of different layers can be derived by this technique.

Aside from producing mass spectra of the sample region, images can also be produce as well. These images are a pictorial method of displaying the ions present at the surface and show their distribution in the scan area. This is possible because of the way data is collected and processed. As each area is exposed to primary ions the secondary ions produced are detected and identified. The specific area of the scan area corresponding to the secondary ions detected is recorded and displayed

pictorially.

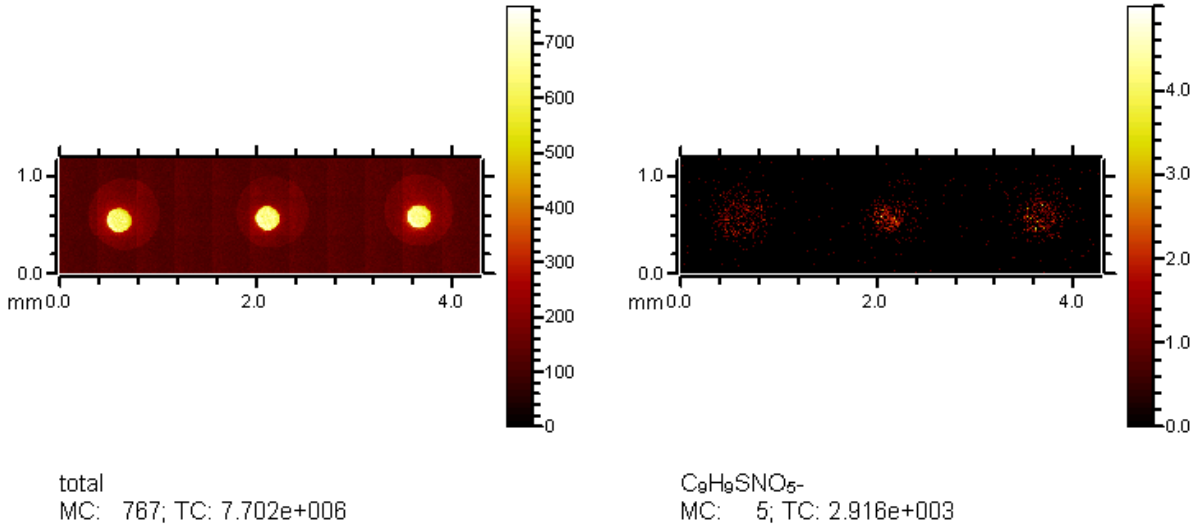


Figure 5 – ToF-SIMS images β-D-thioglucose spots with the $C_9H_9SNO_5^-$ ion image (right) derived from the total ion image (left).

As the scan progresses an image of the sample area is generated. This image is called the total image as it contains the total amount of all ions. Afterwards, the ion peaks of interest ($C_9H_9SNO_5^-$) can be displayed pictorially which ignores all other ions present. What is left is the image of that specific ion showing its distribution. In Figure 5 we can see parallel vertical lines 0.2 mm apart on the left image. These are not due to the sample surface's chemistry but more to do with the way the sample is ionised along and that the image is made up of smaller images stitched together. Sometimes the sample isn't electro conductive (e.g. insulating) or the charge varies across the surface. This alters the amount of secondary ions produced across the surface. An electron flood gun is used to balance the charge across the surface. This is called charge neutralisation. The ion gun which produces primary ions only exposes a small area to primary ions. The ability for the electron gun to neutralise

the charge is strongest at the centre of these exposed areas. At the very edge of the exposed area the electron guns charge neutralisation performance decreases leading to a gridline effect on the scan area. This effect isn't really visible unless there are large regions of uniform ion distribution which is more likely to occur on clean surfaces and total ion images.

### 3.2 Experimental Procedure for ToF-SIMS Data Acquisition

Before ToF-SIMS can be carried, preparation was done to ensure the best results. After the slide(s) were prepared they were left to dry in a desiccator. ToF-SIMS analysis is carried under a high vacuum and liquids on the surface would evaporate as the pressure is reduced. Once the slide is ready for analysis it must first be placed on a stage holder, a component of the ToF-SIMS equipment that holds the sample in place within the vacuum. Nitrile gloves can contaminate the surface. Use of polyethylene gloves will prevent surface contamination. However great care should still be used to ensure direct contact with the slide surface doesn't occur. Adhere the slide to the surface using pins, brackets etc. Insert the stage holder into the transfer chamber and reduce the pressure within the chamber to around $1 \times 10^{-2}$ mbar before transferring the stage holder to into the sample chamber where the pressure is further reduced to around $1 \times 10^{-6}$ mbar. The stage holder's position within the sample chamber could be controlled remotely in the x,y and z directions. The glass slide is a good insulator so charge neutralisation steps were incorporated. The scan area and resolution was chosen

followed by the charge mode which is either positive or negative. Once a scan is complete in one charge mode it is repeated in the other.

### 3.3 Data Processing using ToF-SIMS

Before data processing took place mass calibration of the spectra were carried out. The positive mode spectra were calibrated with $H^+$ and $Na^+$ because they are easy to locate on a mass spectrum and no other ions are similar in mass. Afterwards the spectra were then calibrated against $CH_2^+$, $C_2^+$, $C_3^+$, and $C_4^+$ and their deviations were checked. If these ions had deviations below 40ppm then it can be concluded that the spectra was properly calibrated. The same was done to negative spectra where $H^-$, $O^-$ were used and calibrated against $CH_2^-$, $C_2^-$, $C_3^-$, and $C_4^-$. After calibration a quick scan is carried out across the spectra in order to check peaks that should be present and seeing how accurately the software identifies the peaks. This is a useful practice to have because ToF-SIMS of a single array can yield a tremendous amount of data which can take weeks to months to fully analyse. Prudent searching of peaks related to the scope of the analysis is important to save time. The unit 'ppm' or parts-per-million are used for measuring the closeness of an observed mass/charge value of an ion to the actual mass/charge ratio of that ion. Electrons have a mass of $9.12 \times 10^{-31}$ kg, which will add onto the observed mass detected. Calculating ppm is done with the following equation:

$$ppm = \frac{Observed\frac{m}{z} - Exact\frac{m}{z}}{Exact\frac{m}{z}} \times 1000000$$

After mass spectral calibration, if the ppm value is small enough then the difference can be attributed to the addition of electron mass. If the difference is too high then electron mass cannot be used as a way to explain the difference in mass. Therefore the selected ion cannot be correctly assigned and/or recalibration of the spectra is required.

# 4. Experimental Procedures

## 4.1 Analysis of the Commercially Acquired Amine Coated Slides

The first analysis was with the commercially acquired amine coated surfaces (GAPS II Corning, Bar-coded) from Sigma Aldrich. The main aim of this quick analysis was to simply ensure the slides were made to the quality required. Area scans of ~10 × 10mm were done to ensure there was indeed an amine layer on the surface and that it was uniformly distributed throughout the surface. The results are shown in *Section 5*. A quick fluorescamine assay was also carried out by dipping the amine coated slides in a fluorescamine solution. Fluorescamine reacts with the primary amino groups on the slide surfaces forming fluorescent compounds which were be detected at the 420-620nm range using fluorescence spectroscopy.

## 4.2 Analysis of Maleimide Functionalised Surface

After ensuring the amine coated surface are indeed at the required level of quality, a procedure for attaching maleimide groups onto the surface of the amine coated slides was carried out. The procedure was derived from *Scurr et al*[5]. Below is a table of the required reagents and equipment.

| Reagents | Equipment |
|---|---|
| 6-maleimidohexanoic acid N-hydroxysuccinimide ester (EMCS) | 30 Brand New Beakers* |
| Dimethylformamide (DMF) | Coplin Jar - Brand New |
| Diisopropylethylamine | Falcon Tubes |
| Ethanol | Aluminium Foil |
| Pure Water (HPLC Grade) | Vacuum Desiccator – (No Silicone Grease) |
| | Slide Holders/Mailers |
| | GAPS II Corning, Bar-coded Amine Coated Slides |

*Surface chemistry can be greatly altered with the presence of even small quantities of contaminants. Therefore every reagent and equipment used was completely brand new except for the HPLC Grade water and Ethanol.

Producing the maleimide functional slides occurred in two main steps.

31mg ($1 \times 10^{-5}$ mols) of EMCS was added into a beaker. EMCS powder was dissolved in DMF until complete dissolution has occurred. 1.25ml (2.5% v/v of 50ml) of diisopropylethylamine was then added to the solution. More DMF is added until the 50ml mark was reached. 5 amine coated slides were inserted into the coplin jar.

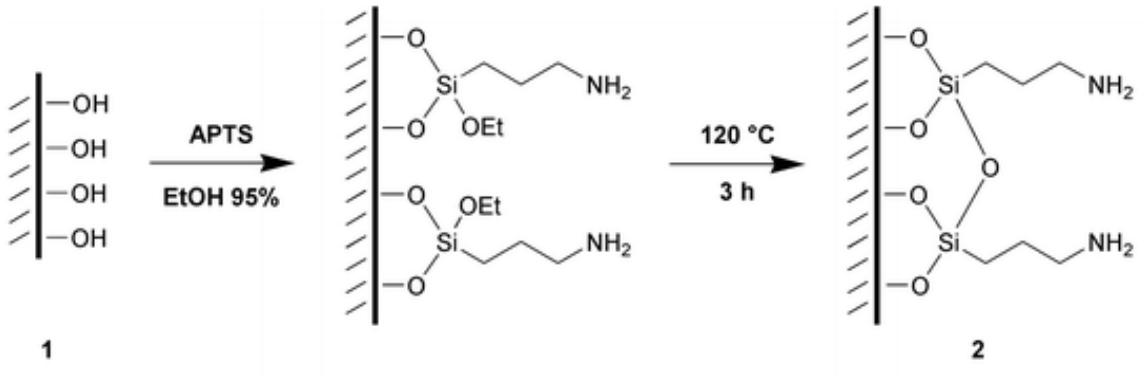


Figure 6 –Synthesis of Amino silane glass slides[26] such as the GAPS II Corning, Bar-coded Amine Coated Slides from Sigma Aldrich[19].

The slides were inserted with the bar-code at the top. The jar lid was placed on top and the jar was wrapped in aluminium foil. The reaction was allowed to continue at room temperature for 24 hours.

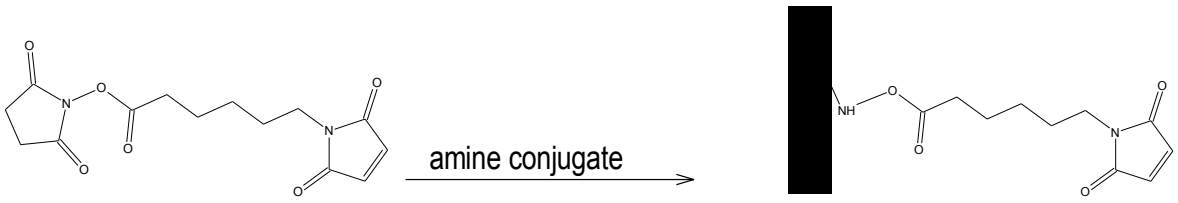


Figure 7 – Reaction scheme of EMCS with anime coated slide surface producing a maleimide layer.

After the reaction has progressed for 24 hours the aluminium foil was removed and the EMCS, DMF, diisopropylethylamine mixture was poured into a falcon tube for future use. 50ml of Ethanol was poured into 15 beakers and 50ml of HPLC grade water into another 15 beakers. Each slide was rinsed three times in ethanol and then three times in water and then dried under using a stream of pressurised nitrogen gas. Fresh ethanol was acquired on site from the University of Nottingham chemical stores and was only used for surface chemistry work. The HPLC grade water was also acquired on site from an electronic water purifier. The slides were placed into a fresh slide mailer ensuring the lid was not completely sealed. The slide mailer and opened desiccator were placed into a glove box and pumped with argon. The slide mailer was placed inside the desiccator for storage and future use. The time between completion the storage of the maleimide coated slides and surface analysis was 3 days and a further two weeks passed until the glycan microarray was produced and analysed.

### 4.3 Array Printing of β-D-thioglucose on Maleimide Coated Slide

A commercially available thiolated sugar from Sigma Aldrich called β-D-thioglucose in salt form was acquired which has the following structure:

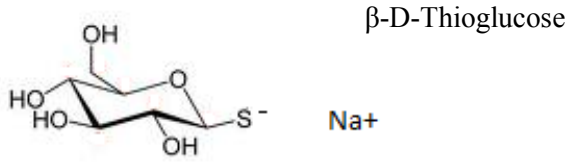


Figure 8 - Structure of the commercially acquired β-D-thioglucose from Sigma Aldrich.

Investigations into the effects of PBS on spot distribution, shape and other characteristics were carried out. PBS is commonly used in sugar chemistry because it maintains the necessary pH for thiol-maleimide reactions to take place while suppressing others. However PBS has been found to form salt concentrations within the centre of spots preventing maleimide-thiol reactions from taking place locally[5], restricting thiol-maleimide reactions at the edge of the spots, and resulting in a glycan ring after rinsing. Because β-D-thioglucose was in the salt form it is possible that the sodium present may cause some of the same effects seen when PBS is used in water spots. However other ions in PBS like $K^+$ and $Cl^-$ should not be present in the water spots.

In order to fully investigate the effects of PBS on spot characteristics the spots were subjected to different variables to see which characteristics were more affected than others. These variables include: β-D-thioglucose concentration, spot volume, humidity during spotting and the use of HPLC

grade water instead of PBS. The concentration of PBS was kept constant whenever it was used and more information about its composition is shown in Table 1.

Table 1: Table of the PBS components at their respective concentrations.

| Salt | Concentration (mmol/L) | Concentration (g/L) |
|---|---|---|
| NaCl | 137 | 8.01 |
| KCl | 2.7 | 0.20 |
| $Na_2HPO_4 \cdot 2\ H_2O$ | 10 | 1.78 |
| $KH_2PO_4$ | 2.0 | 0.27 |
| pH | 7.4 | 7.4 |

Ions such as $Na^+$, $K^+$ and $Cl^-$ are more readily ionisable than most other elements and ionic compounds during ToF-SIMS analysis and produce more secondary ions in disproportion to the amount found on the surface. This is known as the matrix effect[23]. On a typical mass spectrum we cannot conclude that because one peak of a particular ion has a higher intensity than another, that it must be present at a higher concentration on the surface without taking the matrix effect into consideration. If a particular spectra had a higher $Na^+$ peak than $CH_3^+$ for example we cannot say that there must be more $Na^+$ ions than $CH_3^+$ ions because $Na^+$ is more ionisable and produces more secondary ions. Typically ions which are electropositive such as $Na^+$ and ions which are electronegative such as $Cl^-$ tend to be affected more by the matrix effect.

# 5. Results and Discussion

## 5.1 Results of the Analysis of the Commercially Acquired Amine Coated Slides

The top spectrum presented in Figure 9 is from commercially available amine coated borosilicate slides. The bottom spectrum in Figure 9 is an untreated borosilicate slide. Both spectra were acquired from the surface analysis of the amine coated slides in negative ion mode.

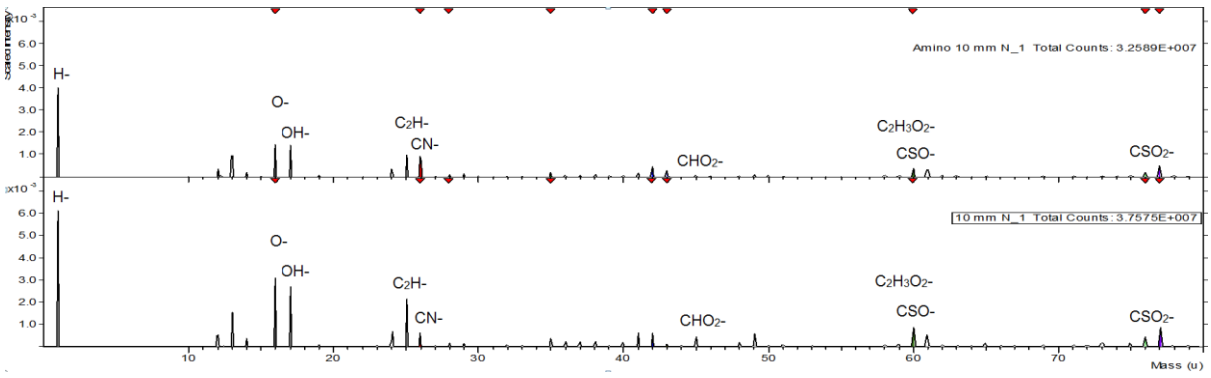


Figure 9 – Negative ion mass spectra of a borosilicate amine coated slide (top) and a plain borosilicate glass slide (bottom).

Several distinct peaks have a lower intensity after amine coating such as $C_2H^-$ (mass = 25) and $CSO^-$ (mass = 60) as shown in Figure 9. Secondary Ion Mass Spectroscopy (SIMS) involves primary ions striking the surface providing it with kinetic energy. If the energy provided is enough, electrons within the atoms are released producing secondary ions as a result of primary ion bombardment. The top 10nm of the surface is energetically excited but secondary ions are only detected from the very top 1-2 nm where their mobility is less restricted by atoms above them[27]. Coating the surface of a glass slide causes a reduction in intensity of the glass constituents below the coating for this reason. This

also explains why peaks indicative of an amine coated slide surface have a higher intensity on the top spectrum in Figure 9 and 10 such as $CN^-$ (mass = 25). The amine layer does not prevent primary ions from reaching the glass surface. Instead the amine layer is preventing some of the secondary ions from leaving the surface and being detected by the mass analyser.

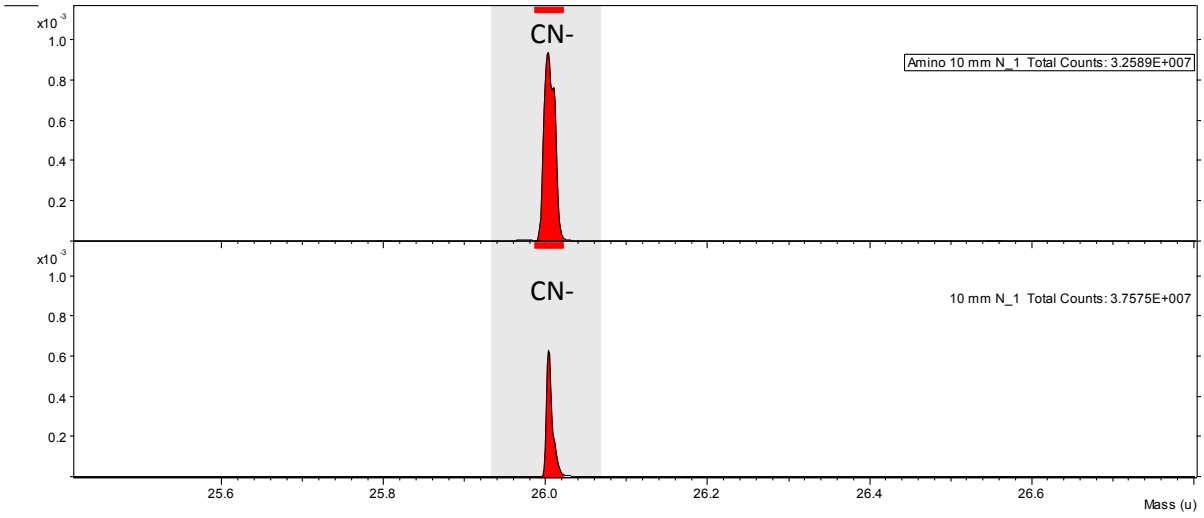


Figure 10 – Negative ion $CN^-$ peaks on borosilicate amine coated slide (top) and a plain borosilicate glass slide (bottom).

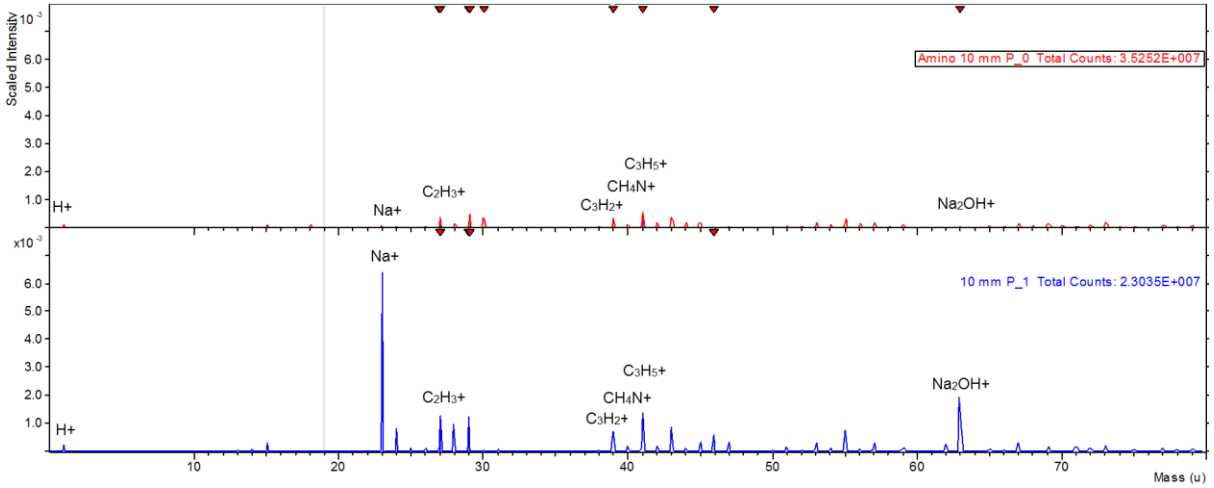


Figure 11 – Positive ion mass spectra of a borosilicate amine coated slide (top) and a plain borosilicate glass slide (bottom).

Peaks which have a higher intensity in Figure 9 are more likely to be attributed to the amine layer and not the glass surface such as the $CN^-$ peaks in Figure 10. The same can be said of peaks that are lacking in one spectrum such as the $Na^+$ peaks in Figure 11. Sodium is easily ionised and even at small quantities it may saturate the detection range of the detector during ToF-SIMS analysis. The lack of $Na^+$ ions in the amine coated slide suggests that the slides were treated and cleaned thoroughly which is expected from commercial products.

Analysis of borosilicate glass slides and borosilicate powder have shown that there is no significant amount of $CN^-$ in its composition[28]. The $CN^-$ ions found on the plain borosilicate glass in Figure 9 was must therefore be a surface contaminant. $CN^-$ from atmospheric ammonia may have reacted with the surface. This would explain why most of the areas of the plain slide have a uniform distribution of $CN^-$ ions.

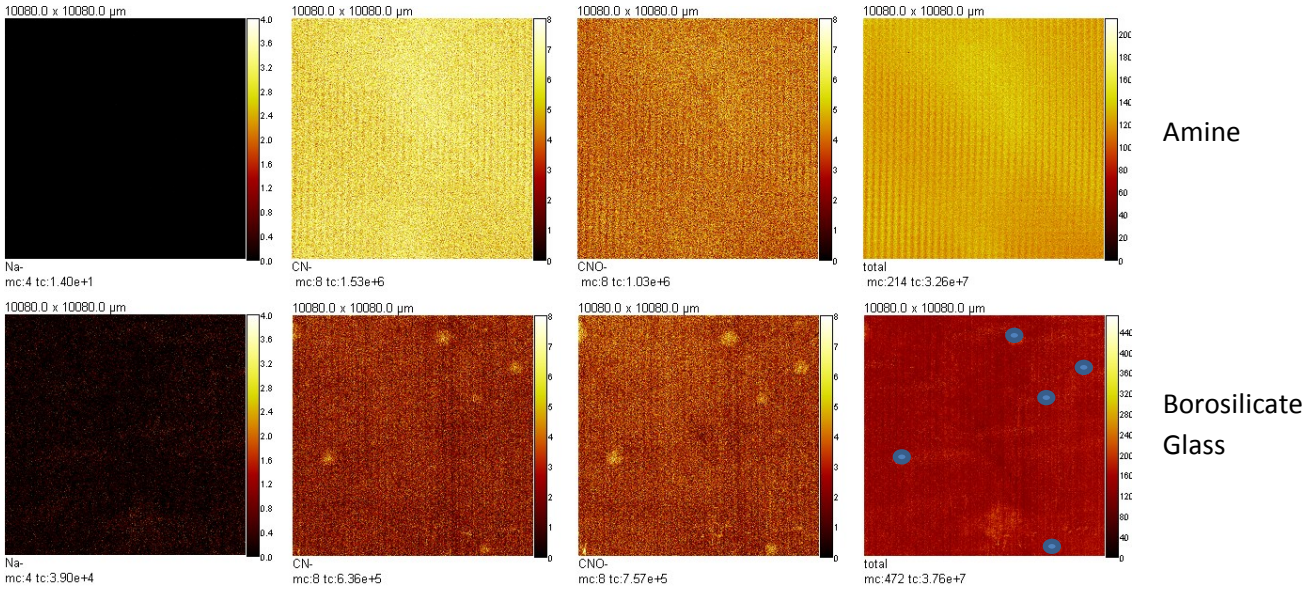


Figure 12 – ToF-SIMS images of $Na^-$, $CN^-$, $CNO^-$ and the total images on the amine coated slide (top) and their respective images on the plain borosilicate slide (bottom).

The top 4 images in Figure 12 are from the amine coated surface which looks more uniform and lacks any detectable $Na^+$ compared to the blank borosilicate glass which has surface contaminants. One thing to note is the apparent patchwork pattern seen in the images, especially in the amine coated slide images. These are artefacts generated by the electron flood gun not completely equalising the charge around the scan area. Usually they are more visible in image scans where the surface is more uniform. The scan area was 256µm by 256µm squares. Therefore the edges of the scan area receive less charging that the centres. The sample is analysed by collecting data from one area then moving across to the next 256µm by 256µm area slowly patching the total image together as it scans. Ways to reduce this effect are smaller scan areas which causes longer scan times or bigger scan areas which leads to fewer lines but lower image resolution. $CN^-$ and $CNO^-$ ions are found in an

uneven distribution on the untreated borosilicate slide surface compared to the amine coated slide in Figure 12. Their relative intensities are also lower than on the amine coated slides which means these two ion species are ion fragments from the amine coating itself. There are small regions of high intensity $CN^-$ and $CNO^-$ regions on the untreated slide which are marked in blue circles in the total image. Their presence is best explained as contaminant deposits.

Analysis of the amine coated slides was also performed by applying a solution of fluorescamine onto the surface. Fluorescamine reacts with primary amine groups found on the surface of amine coated slides forming an adduct[29]. To the naked eye an amine coated slide surface would turn to a light blue colour. This would show that the acquired slides were indeed amine coated. However to ensure the surface was clean and the amine surface was uniform a surface analysis technique such as ToF-SIMS would be needed.

### 5.2 Results of the Analysis of the Maleimide Functionalised Slides

After the maleimide slides were produced dried and stored away, one slide was removed from the slide mailer and the others were repacked following the storage procedure used previously. This slide was analysed using ToF-SIMS to ensure maleimide functionalization had occurred. One possible mass spectra fragment would be the maleimide group itself which may exists in two fragments of

$C_4H_3NO_2^-$ or $C_4H_2NO_2^-$ with masses of 97.09 and 96.01 (m/z) respectively, as shown in Figure 13.

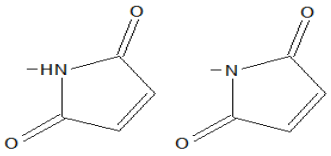


Figure 13 – Structure of 97.09m/z and 96.01m/z ions showing maleimide presence on EMCS treated slides.

The first fragment compared is the smaller mass ($C_4H_2NO_2^-$) of 96.01 m/z which is shown below.

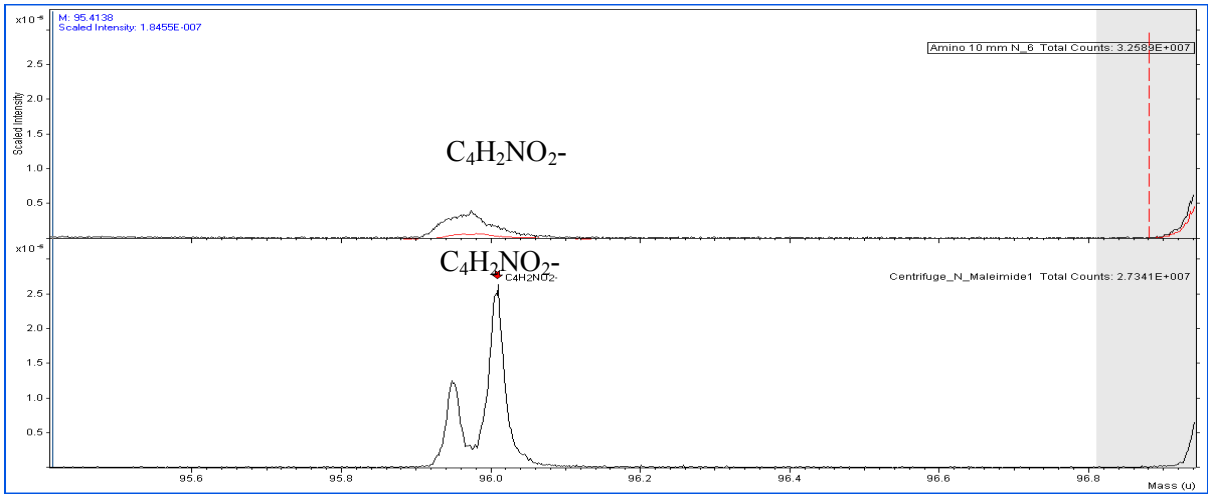


Figure 14 – Negative ion $C_4H_2NO_2^-$ peaks on borosilicate amine coated slide (top) and a maleimide coated slide (bottom).

There is a well-defined peak in Figure 14 of the maleimide spectra at 96.01 m/z when compared to the less defined and lower intensity peak in the amine coated slide. This is a good indication that the surface of the treated slides had been maleimide functionalised successfully. Another possible negatively charged fragment from the maleimide linker structure could have the formula: R-$COO^-$ One such fragment has the chemical formula of $C_4H_5O_2^-$ as shown in Figure 15.

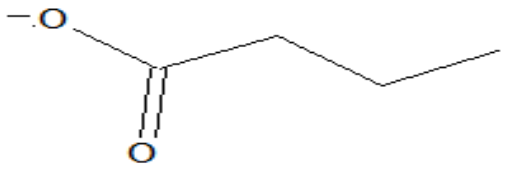

Figure 15 – Molecular structure of $C_4H_5O_2^-$.

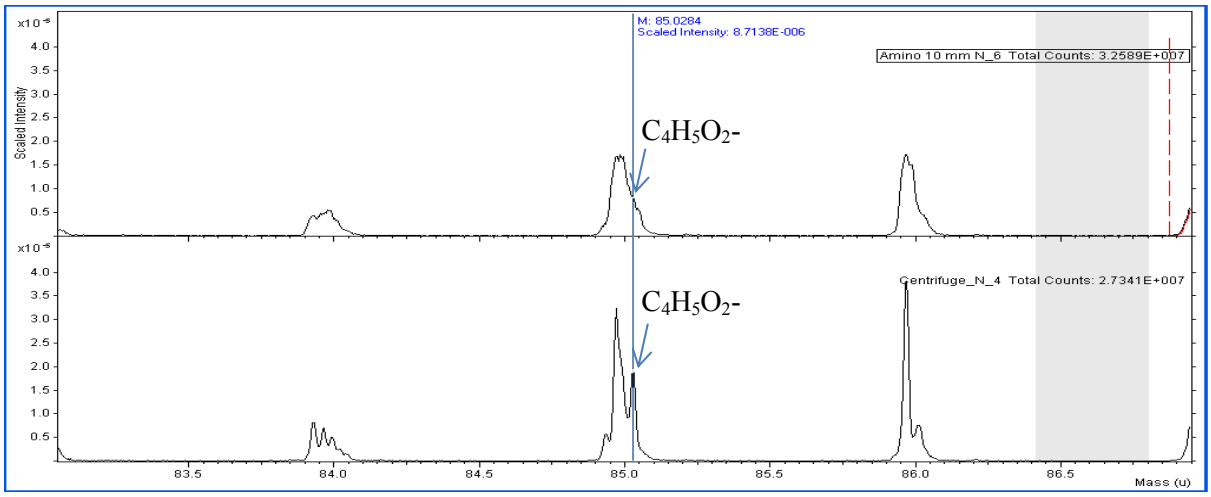


Figure 16 – Negative ion $C_4H_5O_2^-$ peaks on borosilicate amine coated slide (top) and a maleimide coated slide (bottom).

Again in Figure 16 we see a more distinct peak indicative of a maleimide coated surface in the bottom spectrum. Analysing the ion distribution images derived from SIMS analysis confers the benefit of seeing the distribution of the ions of interest. Even if peaks have similar intensities on spectra they may have different distributions throughout the scan area.

The images in Figure 17 below shows six comparative pixel images, each representing an ion fragment. Some of the images are very similar while others are drastically different. The top sets of

images are from the commercially acquired amine coated slides while the bottoms set are from the maleimide functionalised slides.

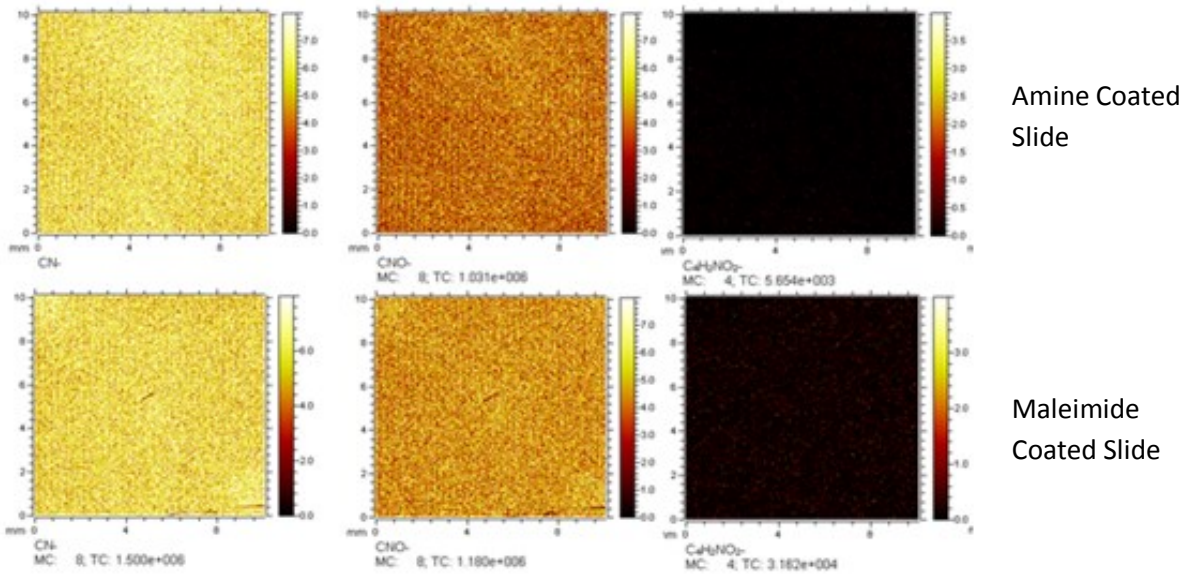


Figure 17 – ToF-SIMS images of $CN^-$, $CNO^-$ and the $C_9H_9SNO_5^-$ total images on the amine coated slide (top) and their respective images on the maleimide slide (bottom).

The relative intensity of $CN^-$ in both slides in Figure 17 is very similar. The structure of the maleimide linker only has one C-N bond in which the nitrogen atom is part of the maleimide group. Therefore it would be rather difficult to break this bond to produce $CN^-$ fragments. The more likely reason is that these detected $CN^-$ ions arise from amine groups that did not react with EMCS during the lab procedure, which would explain why the intensity of the $CN^-$ fragments is only slightly higher in the maleimide image. This is further backed up by the $C_4H_2NO_2^-$ images. In both images the intensity is low. However the intensity of $C_4H_2NO_2^-$ is higher in the maleimide functionalised slides.

This shows that maleimide functionalization has occurred but perhaps not to a high degree. To prove this XPS would have to be carried out in order to quantify the actual amount of $C_9H_9SNO_5^-$. Reasons why $C_9H_9SNO_5^-$ may have occurred at a low yield could be due to factors such as steric hindrance, or that the maleimide group does not readily form this particular fragment upon ionisation. Also the matrix effect can play a factor here in which the maleimide surface is not readily ionisable when compared to $CN^-$ which is more readily ionisable from the amine layer. The good thing is that the image for $C_4H_2NO_2^-$ is uniform showing a good even distribution. Lastly there is an increase in the intensity of the $CNO^-$ image in Figure 17. The images look very similar to each other but the total counts of the maleimide slide has increases to $1.18 \times 10^6$ from $1.031 \times 10^6$ in the amine coated slides. Before the lab procedure the surface of the amine coated slides would have been R-$NH_2$. After the procedure it would have been R-NH-O-C-R. Within that arrangement is a possible $CNO^-$ fragment. Remembering that the increase in $C_4H_2NO_2^-$ in Figure 17 was significant from a total count of $3.162 \times 10^3$ in the maleimide slides from $5.654 \times 10^4$ in the amine coated slides (nearly 10 fold) but that the intensity of the image was low will mean that the levels of $CNO^-$ should also increase but only slightly. This is what we are seeing with these images.

### 5.3 Results from the Analysis of the β-D-thioglucose Microarray

The maleimide slides were analysed and then used to produce β-D-thioglucose spots. The spots are what are left after the sessile drop on the maleimide slides during printing evaporates. Comparision of this state, where all the solute is present in the spot, to the post rinsed state, when the excess non-covalently bonded materials was assumed to have been rinsed off [30]. The composition of the spot will be β-D-thioglucose-maleimide interactions by covalent bonding, unreacted β-D-thioglucose and in some cases PBS salts. The β-D-thioglucose spots were produced under different variables caused by different concentrations of β-D-thioglucose, different volumes of the drop solution and the use of PBS. The first variable that was monitored was the change in spot size in relation to the concentration of β-D-thioglucose. Spot size was measured by using a retrospective intensity line scan across the image of the spots. This displayed a graph, shown in Figure 18 that correlated to the intensity detected across an area. Initially the graph line is even due to the uniform intensity of the maleimide surface. As the line scan crosses over the spot the graph line will change due to an increase or decrease in the intensity of the image. The graph line returns to normal once it has gone across the spot. The distance across the x-axis during this is the same as the spot size.

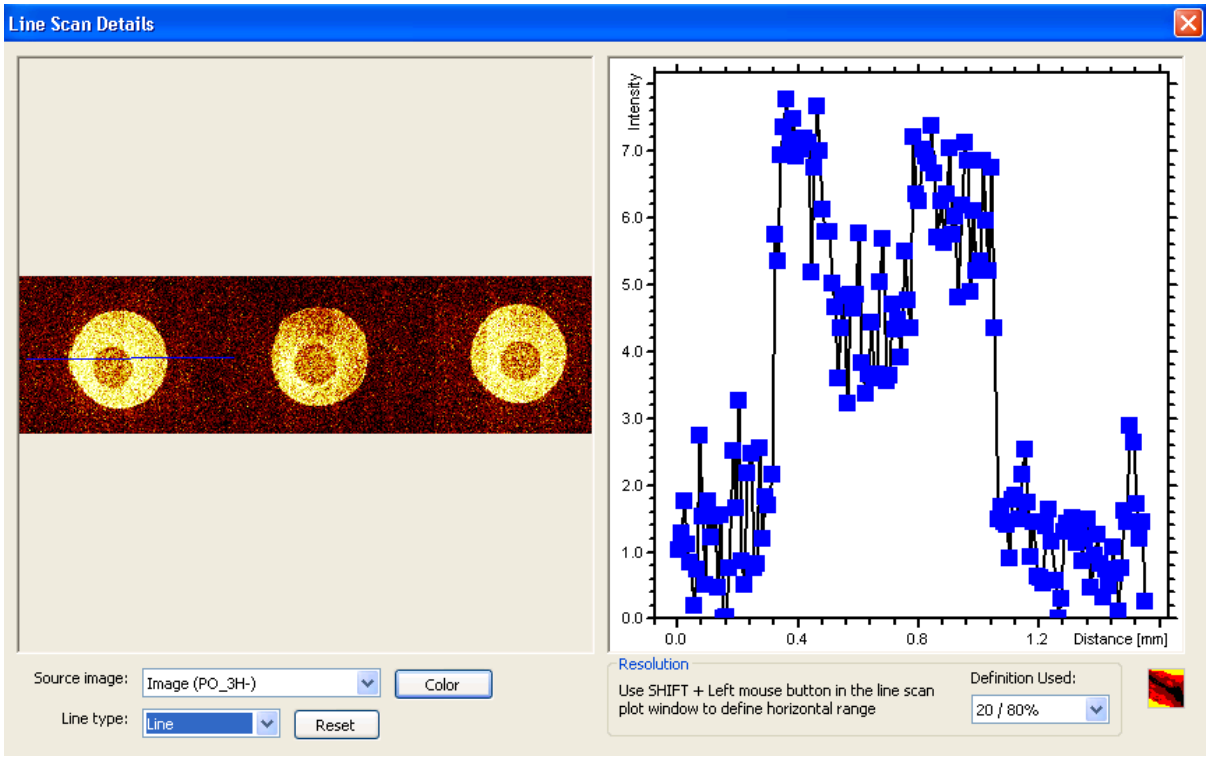


Figure 18 – Example of how the Line Scan Editor tool can be used to accurately measure a spot's diameter. This particular ion is $PO_3H^-$ from the 200 mM β-D-thioglucose PBS spot.

The above spot in Figure 18 has a line drawn through its maximum horizontal diameter and the profile graph of intensity vs. distance is shown to its right. The distance from where the intensity changes and returns to normal is between 0.4 and 1.1mm (the spot size is 0.8mm in diameter).

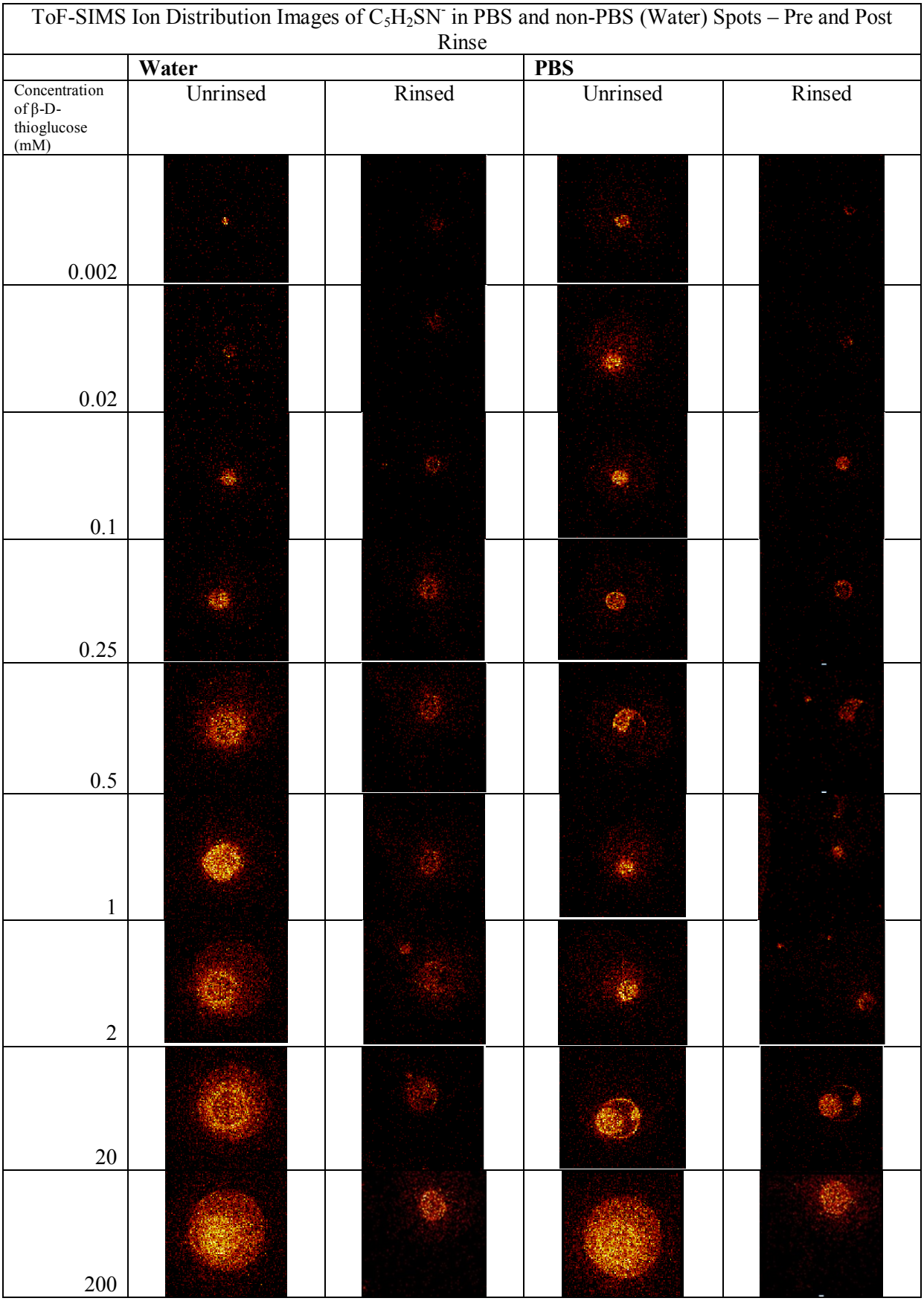


Figure 19 – ToF-SIMS images of unrinsed and rinsed β-D-thioglucose PBS and water spots for $C5H2SN^-$ from 2.32nl sessile drops.

Figure 19 shows ToF-SIMS images of $C_5H_2SN^-$ ion distribution within the spots on the maleimide functionalised glass slides. This ion fragment fulfils the criteria to show its origin is from a successful β-D-thioglucose/maleimide surface complex. The criteria are that it has an S-N bond within its structure which is only possible from a β-D-thioglucose /maleimide surface covalent bond via the thiol group on the sugar and it's found at a higher intensity within the spots when compared to the regions outside the spots. The images are shown in descending order of β-D-thioglucose concentration from 0.002mM to 200 mM and arranged in columns groups. The first two columns on the left are spots formed from drops that contained no PBS where the left is unrinsed and the right is rinsed. The last two columns are spots from drops that contained PBS.

As the concentration of β-D-thioglucose decreases the ion distribution of $C_5H_2SN^-$ also decreases as well. This is true for both PBS and non-PBS containing spots. The presence of β-D-thioglucose leads to larger sessile drops in terms of diameter because it causes the surface tension of the drop to the maleimide surface to decrease while it is on the surface. As a result, higher concentrations of β-D-thioglucose lead to lower surface tensions and therefore larger spots.

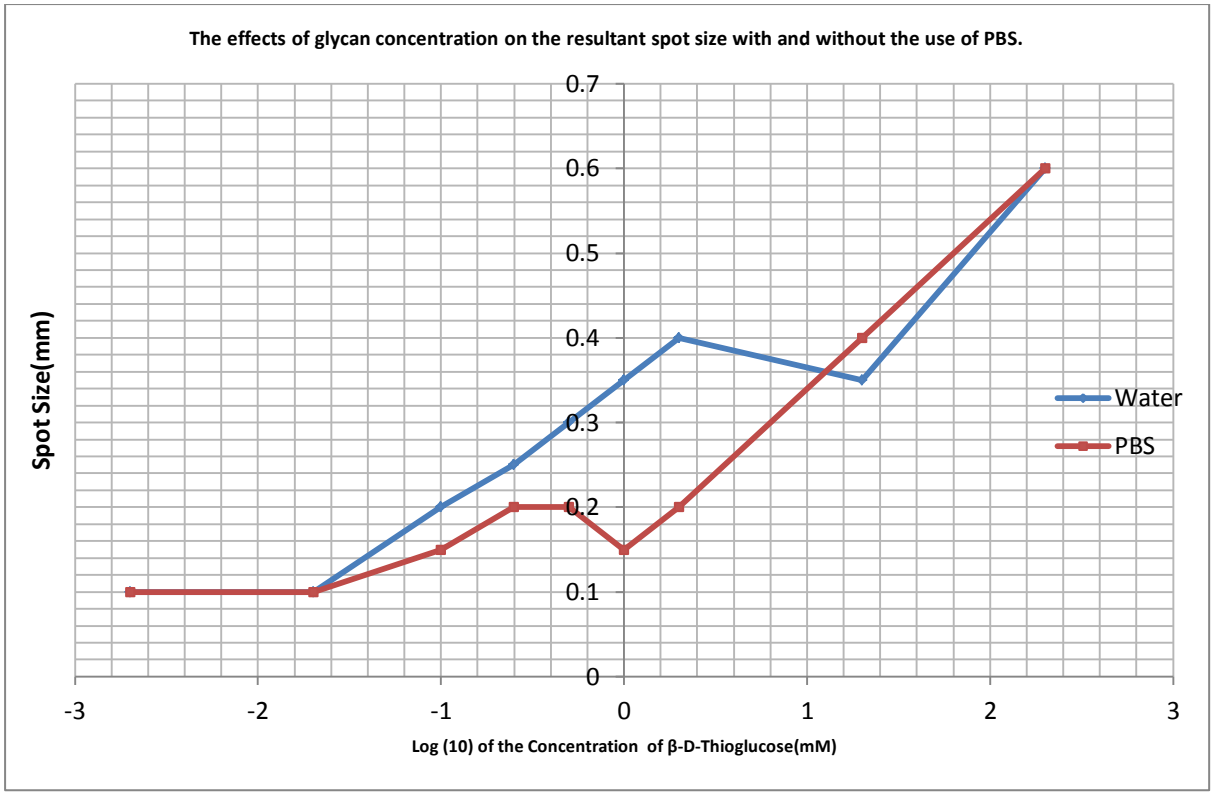


Figure 20 – Graph of the Log (10) of the concentration of β-D-thioglucose (mM) against spot size (mm) post rinse.

The graph in Figure 20 shows how the presence of PBS affects the spot size. At very low concentrations of 0.002mM β-D-thioglucose, the effects of PBS are negligible and the spot sizes are the same for PBS and non-PBS containing spots. This persists until 0.02mM where the non-PBS containing spots are larger than the PBS containing spots at respective concentrations. At higher concentrations of 20mM and 200 mM the effects of PBS diminishes as the spot sizes become more equal again when comparing PBS to non-PBS spots. It's possible that due to the fixed volume of the sessile drops, increasing the concentration of β-D-thioglucose past a certain point no longer affects the drop diameter because the critical surface tension may have been reached. At this point complete wetting occurs regardless of solution composition and is only dependant on the solid surface tension. The spots disperse as much as they can on the surface leading to similar spot sizes with or without the

presence of PBS. Increasing the volume would allow for a larger dispersion and therefore a larger spot size[31].

The salts present in the non-PBS spots are contaminants from the microarray production procedure. This is because these salts are not present on the amine coated slides. The salts may have as part of the β-D-thioglucose sugar composition. Rinsing the spots deposited from non-PBS drops leads to a decrease in the intensity of $C_5H_2SN^-$ images. This indicates that some of the sugar compounds which were bonded to the maleimide surface via the thiol group were washed away during rinsing. Once the microarray was produced it was stored for about 2 weeks unrinsed before analysis. Afterwards it was rinsed and analysed again 2 days later. It is possible that some degradation took place while the slides were stored which would explain why the rinsed water spots are smaller than their unrinsed counterparts. The same observation is seen with the PBS spots as well. It may very well be that greatly reducing the time between microarray production and analysis will lead to far less removal of β-D-thioglucose-maleimide compounds on the glass slide surface. However it's more likely that the loss of intensity in the rinsed samples is due to excess material being washed off. *Scurr et al* [5] received a microarray that had been prepared using PBS. They stated that $C_2H_3O^+$ was indicative of their saccharide distribution. The procedure used to produce the microarrays in this project was based on their procedure, including the use of maleimide functionalised glass slides.

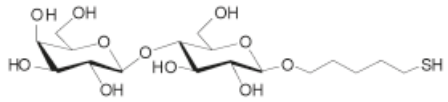


Figure 21: Galactose (β1-4) glucose which is one of the saccharides used by *Scurr et al* 2011. The ion distribution images are shown below in Figure 22.

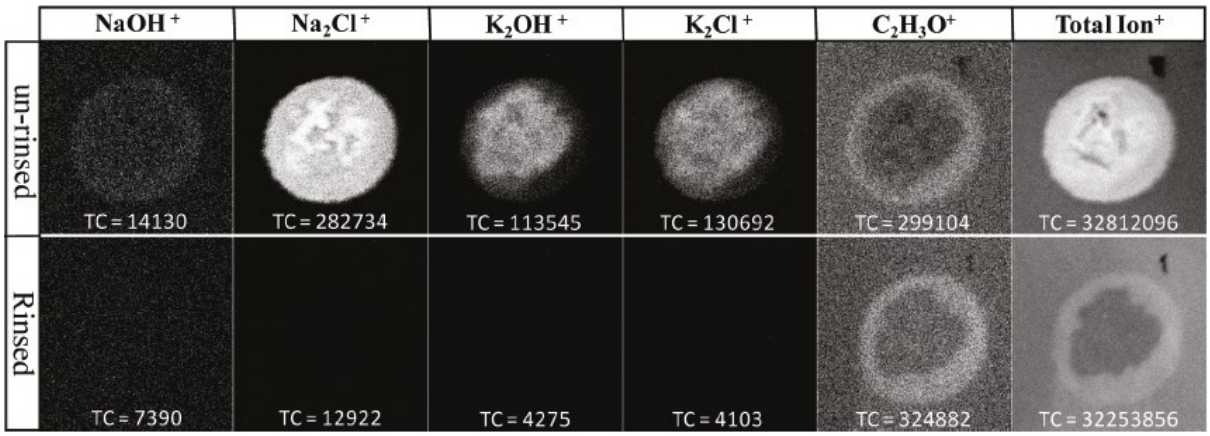


Figure 22: $C_2H_3O$+ ion distribution which was indicative of galactose-(β1-4)-glucose distribution in *Scurr et al*[5] including some salts from the use of PBS and the total ion. The top images are unrinsed spots while the bottom images show the ion distribution after rinsing.

Pre and post rinse images of their spots show that galactose-(β1-4)-glucose had only reacted with the maleimide surface around the spot edge and not at the spot centre. The unrinsed total ion shows that there is some material at the spot centre. This correlates with their conclusion that the material is the PBS ions ($Na_2Cl^+$ $K_2Cl^+$ etc.) which after rinsing are removed leaving only the saccharide within the spot at the spot edge. It was concluded that the use of PBS prevented galactose-(β1-4)-glucose from reacting with the maleimide surface. Investigations of whether the use of PBS prevents the saccharide from forming a uniform distribution within the spot is one of the reasons similar chemistry was used to form microarrays based on *Scurr et al*[5] where some of the spots were produced from sessile drops that do not contain PBS.

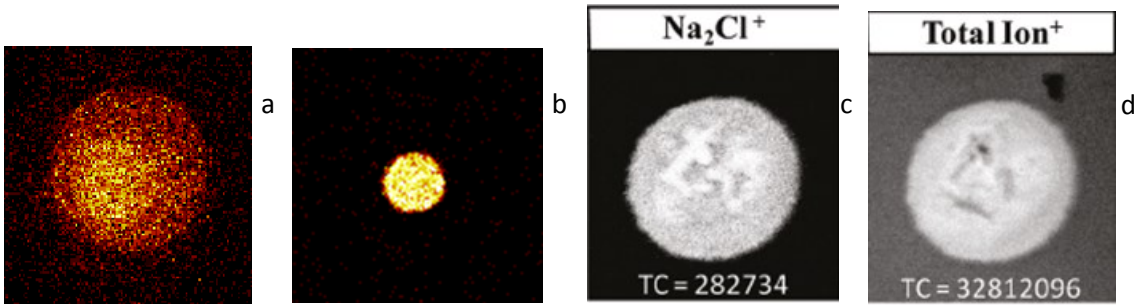


Figure 23 – Unrinsed β-D-thioglucose $C_5H_2SN^-$ ion distribution (a), unrinsed β-D-thioglucose $Na_2Cl^+$ ion distribution (b), unrinsed galactose-(β1-4)-glucose $Na_2Cl^+$ from Scurr et al[5] (c) and the same spot at total ion (d). All are at a concentration of 2mM of their respective sugars.

The biggest difference between the produced spots (a,b) in Figure 23 and the images from the literature (c,d) are the differences in the ion distribution of $Na_2Cl^+$. The $C_5H_2SN^-$ ion distribution covers a larger area than the $Na_2Cl^+$ ion distribution for the spots produced (a,b) compared to those from the literature (c,d). While the $Na_2Cl^+$ ion distribution covers the exact size area as the corresponding total ion for the spot images from the Scurr literature[5]. This is true for other ions present from the literature such as $K_2OH$ and $K_2Cl^+$ in which their ion distributions size is the same as the total ion distribution.

For the of β-D-thioglucose spots, the presence of PBS in the solution does not affect sugar binding to the maleimide surface and instead what we see is an increase in the intensity of $C_5H_2SN^-$ at the spot centre compared to the spot edge. This could be due to the fact that these two sugars have different structures. While they are both thiolated sugars, β-D-thioglucose is a monomer and its thiol group is the result of a substituted –OH group. Galactose-(β1-4)-glucose is a disaccharide and its thiol group is present on an alkyl linker which substitutes a hydroxyl group. These differences in chemical structure may have led to the drastic difference in the ion distribution of the respective ion which is

indicative of a sugar-maleimide bond. One way to confirm this is to produce spots of galactose-(β1-4)-glucose using the same procedures but without the use of PBS to see if there is any difference. However due to the high costs of synthesizing this disaccharide, this was not possible.

One thing that remains the same is that the PBS components are found mainly at the spot centres after the sessile drop dries. The $Na_2Cl^+$ ion distribution image in Figure 23 (c) from the literature has a more intense region at the centre that is reminiscent of crystallisation of the salt after drop evaporation. This can also be seen with the image (b) from Figure 23 as well. There is a lower intensity of $Na_2Cl^+$ around the spot edge in image (c) from Figure 23 which is not present in image (b) image from Figure 30. So while $Na_2Cl^+$ collects throughout the entire spot when galactose (β1-4) glucose is used it only collects at the spot centre when β-D-thioglucose was used. The procedures used are the same, PBS was used and the spots are both 2mM of their respective sugars. This leaves the sugars themselves as the difference between the two procedures that led to different ion distribution of $Na_2Cl^+$. One possibility is that galactose (β1-4) glucose has a lower solution viscosity than β-D-thioglucose.

When the sessile drop forms on the surface during microarray printing it begins to evaporate.

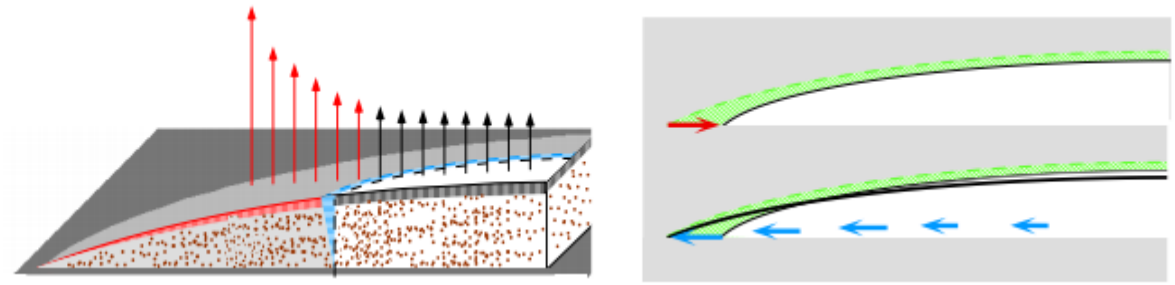

Figure 24- Diagram depicting the differences in evaporation rate due to surface area (left) and the net flow of solution as a result (right).

Due to the shape of the drop, evaporation takes place quicker at the drop edge than at the drop centre. This is because the surface area is highest at the drop edge. At the drop edge the concentration of solutes increases and at the very edge of the drop they precipitate and are left behind if they are saturated [40]. This is shown in the diagrams in Figure 24. The reason saturation is required for deposition is due to another directional flow of dissolved solutes towards the centre of the drop. As the solutes travel towards the spot edge due to quicker evaporation rates at the edge, the concentration of solutes decreases at the spot centre. This in turn causes solutes to flow towards the bulk solution at the spot centre due to entropy of mixing in order to maintain an even distribution of solutes within the solution. When saturation for a particular solute occurs at the spot edge, it leads to precipitation forming a suspension of the previous solute which is left behind as the drop edge recedes. The more viscous β-D-thioglucose solution prevents precipitation of the PBS components such as $Na^+$ and $K^+$ due to the higher amount of intermolecular forces present. As a result the drop evaporates and only the less soluble β-D-thioglucose remains on the surface due to precipitation or chemical bonding until

the drop is much smaller. This may explain why $Na_2Cl^+$ is only found at the β-D-thioglucose spot edges while it's found throughout the spot in the galactose-(β1-4)-glucose spots from the Scurr literature[5].

Looking at Figure 19 we can see the use of PBS doesn't prevent β-D-thioglucose from reacting with the spot centre. In fact there seems to be an increase in the amount of β-D-thioglucose/maleimide interactions at the spot centres which is more apparent after rinsing. This does not mean that Scurr et al, conclusion about PBS was incorrect in that it prevents saccharides from reacting with the spot centre due to the use of PBS. This is because the procedure used was not identical to theirs. The differences include the saccharide used and the use of a thiol linker. The saccharide results they used to draw up their conclusions are on galactose-(β1-4)-glucose which is a disaccharide. The saccharide used here was β-D-thioglucose which is a monosaccharide. Longer chain saccharides usually have lower solubilities than monosaccharides. Starch for example is insoluble in cold water while glucose is soluble in the same environment. β-D-thioglucose being a monosaccharide may have been more soluble and remained in solution even as the drop diameter decreased during evaporation. As the drop receded to where the spot centre would be, the concentration of β-D-thioglucose would have been at its highest promoting higher rates of reaction with the maleimide surface which may explain the higher intensity of $C_5H_2SN^-$ at the spot centre in Figure 23 (a,b). However further research is required to back up this claim.

Another possible reason is because β-D-thioglucose lacked an alkyl thiol linker which is present in galactose-(β1-4)-glucose. Presence of the hydrophobic alkyl linker arm could have decreased the solubility of galactose-(β1-4)-glucose enough to cause it to precipitate out of solution so that by the time the drop had decreased in size sufficiently there was no more sugar dissolved to react with the surface near the resultant spot centre, leaving only the more soluble PBS components still in solution[32]. But like before, this requires further research to substantiate these claims.

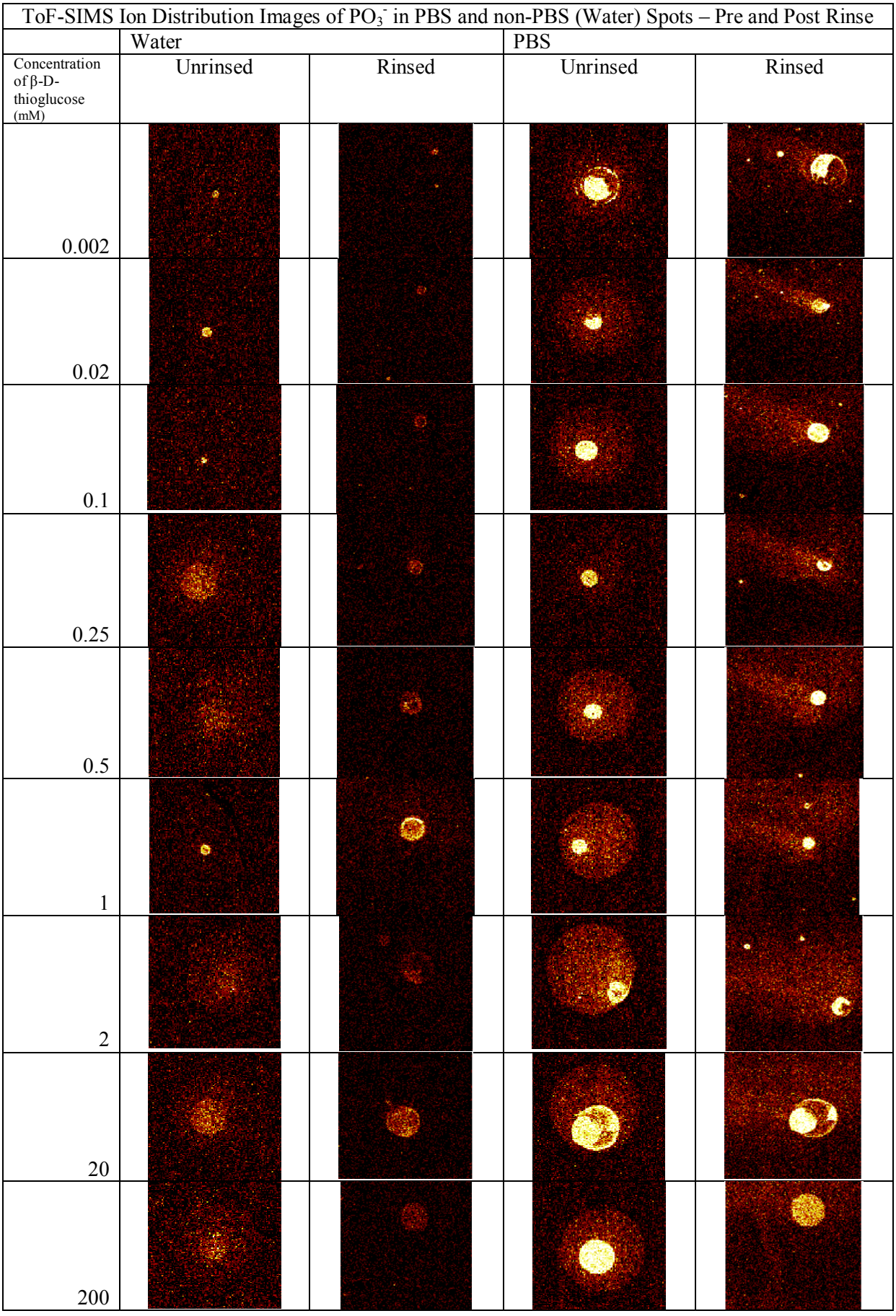


Figure 25 – ToF-SIMS images of unrinsed and rinsed PBS and water spots for $PO_3^-$.

After rinsing there is a comet like distribution of $PO_3^-$ in the PBS spots which is not present in the non-PBS spots. The most likely reason for this is that rinsing was incomplete and not all of the $PO_3^-$ ions were washed away during the rinsing step leaving behind streaks of $PO_3^-$ ions which are all parallel to each other. β-D-thioglucose may be viscous enough to hold some of the $PO3^-$ ions during the rinsing step. To prevent this in the future the rinsing step must be improved. The existing method is to dip the printed slides in water and ethanol three times separately. Perhaps some gentle shaking of the slides coupled with an increased submersion time may prevent this streaking effect seen above. Alternatively sonication which is a technique that is used to subject materials to ultrasound can be used to remove the PBS components and unreacted reagents on the surface. By subjecting the slides to sonication, the intermolecular forces between substances such as $PO_3^-$ with the possibly viscous β-D-thioglucose are broken which increases the rate of $PO_3^-$ dissolution in the water and ethanol used making for a more effective rinsing method[33].

The significant intensity and distribution of $PO_3^-$ in the non-PBS containing spots suggests that the β-D-thioglucose contains $PO_3^-$ ions. Within the water sessile drop during the printing procedure there would be tris(2-carboxyethyl)phosphine (TCEP) at the same mole equivalent as β-D-thioglucose dissolved in water. TCEP is reducing agent that breaks disulphide bonds that may form between two thiolated sugars. The ion distribution of $PO_3^-$ correlates with the concentration of β-D-thioglucose and therefore TCEP. Therefore the introduction of $PO_3^-$ must come from one of these two

reagents. TCEP contains phosphorus but not in salt form. It remains stable under aqueous conditions and so it's unlikely it is the source of the $PO_3^-$ contamination[34]. This leaves β-D-thioglucose as the source of the contamination. Sugars synthesis can require a large number of steps where the pH can fluctuate significantly. Buffer solutions are sometimes used to maintain a constant pH in conjunction with ion-exchange resins[35]. Due to the matrix effect, even if a small amount of $PO_3^-$ remained after synthesis it would lead to a high intensity ion distribution.

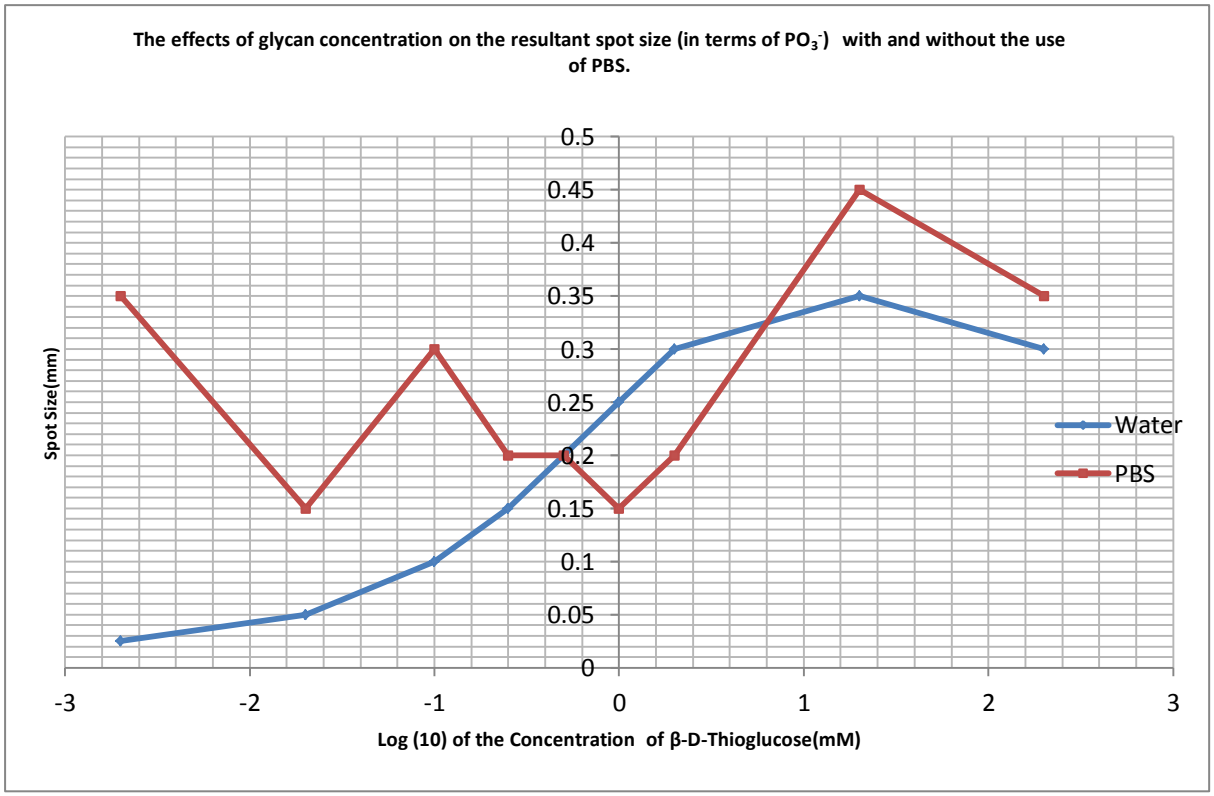


Figure 26 – Graph of Log (10) of the concentration of β-D-thioglucose (mM) against $PO_3^-$ ion distribution (mm) post rinse.

From the graph in Figure 26 we can see that the addition of PBS does not affect the ion distribution of $PO_3^-$ as the concentration of β-D-thioglucose increase. There is no apparent relationship between the additions of PBS, on spot size for different β-D-thioglucose concentrations. When PBS isn't added there is a direct correlation between the ion distribution of $PO_3^-$ and the concentration of β-

D-thioglucose. The amount of $PO_3^-$ is much lower in the water spots and its presence is due to contamination. At these lower amounts of $PO_3^-$ in the water spots, the increasing concentration of β-D-thioglucose decreases the amount of $PO_3^-$ being washed off leading to a higher distribution of $PO_3^-$ as the concentration of β-D-thioglucose increases. To conclude, the higher the concentration of β-D-thioglucose the lower the amount of $PO_3^-$ is washed off. One possibility is that β-D-thioglucose increases the viscosity of the solution is it present in. As the sessile drop dries β-D-thioglucose forms a film on the surface trapping some $PO_3^-$ within the film. Wetting the slide surface during rinsing may not completely dissolve this film which prevents the dissolution of $PO_3^-$ salts.

Unlike the β-D-thioglucose concentration which varied, the concentration of PBS remained the same. There is a higher amount of $PO_3^-$ at the spot centres than the spot edges and even less on the maleimide surface as shown in Figure 25. This is because $PO_3^-$ is water soluble. The sessile drop on the surface would have contained all of the β-D-thioglucose and PBS components dissolved. As the drop began to evaporate different solutes would approach their saturation points and precipitated out of solution.

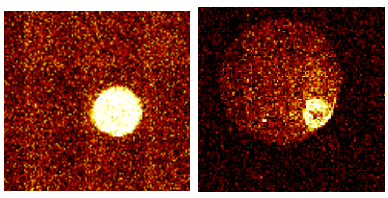

Figure 27 – $K^+$ ion distribution on a 200 mM β-D-thioglucose PBS spot (left) and $PO_3^-$ ion distribution on a 200 mM β-D-thioglucose PBS spot (right).

**Solubility Table**

| Ion | Solubility | Exceptions |
|---|---|---|
| $NO_3^-$ | soluble | none |
| $ClO_4^-$ | soluble | none |
| $Cl^-$ | soluble | except $Ag^+$, $Hg_2^{2+}$, $*Pb^{2+}$ |
| $I^-$ | soluble | except $Ag^+$, $Hg_2^{2+}$, $Pb^{2+}$ |
| $SO_4^{2-}$ | soluble | except $Ca^{2+}$, $Ba^{2+}$, $Sr^{2+}$, $Hg^{2+}$, $Pb^{2+}$, $Ag^+$ |
| $CO_3^{2-}$ | insoluble | except Group IA and $NH_4^+$ |
| $PO_4^{3-}$ | insoluble | except Group IA and $NH_4^+$ |
| $^-OH$ | insoluble | except Group IA, $*Ca^{2+}$, $Ba^{2+}$, $Sr^{2+}$ |
| $S^{2-}$ | insoluble | except Group IA, IIA and $NH_4^+$ |
| $Na^+$ | soluble | none |
| $NH_4^+$ | soluble | none |
| $K^+$ | soluble | none |

***slightly soluble**

| | | Soluble/Insoluble |
|---|---|---|
| a) | AgI | |
| b) | $(NH_4)_2SO_4$ | |
| c) | $Cu(OH)_2$ | |

Figure 28 – A solubility table from the Oklahoma State University AP Chemistry Lecture Notes on Equilibrium in Aqueous Solution[41].

From the solubility table in Figure 28 we can see that in general phosphates are insoluble in aqueous solutions unless they are in an alkali metal salt form or as an ammonium salt. Potassium ions are generally soluble in all salt forms.

$PO_3^-$ has a lower solubility than other PBS components such as $K^+$ because it began to precipitate out earlier as shown in Figure 27. This is why some $PO_3^-$ is present at the spot edge in Figure 27. Figure 27 also shows us the $K^+$ ion distribution in a 200 mM PBS spot. Note that $K^+$ is only found at a significantly higher intensity (from the background) at the spot centre. This means that the local concentration of $K^+$ did not approach its saturated solubility until the drop was much smaller. However the solubility of $PO_3^-$ is low enough that some of it precipitates out when the sessile drop is much larger in diameter. However most of the $PO_3^-$ precipitates out at the spot centre as well.

This is why we see some $PO_3^-$ at the spot edge but a much higher amount at the spot centre. Rinsing the PBS spots leads to a decreased intensity of $PO_3^-$ ions from the spot edge while most of the $PO_3^-$ intensity at the spot centres remains. This does not mean that $PO_3^-$ was not removed from the

spot centre. The distribution of $PO_3^-$ is similar to the $Na_2Cl^+$ found in the literature[5]. The intensity is highest at the spot centre but still found throughout the spot.

Due to the matrix effect some atoms and compounds, especially those containing metals are more readily ionisable due to primary ion exposure during ToF-SIMS analysis. As a result these substances are usually ionised at a level higher than the detection limit of the analyser which effectively leads to a saturation of their ion distribution images. This saturation was present on all images pre-rinse and if enough $PO_3^-$ remains then the regions of high intensity may remain saturated even though most of the ions were washed away during rinsing. This would explain why the ion distribution of $PO_3^-$ decreased around the spot edge where it was not at a saturated level pre-rinsed.

The spots which were formed from drops that contained no PBS have a much lower amount of $PO_3^-$ ions than their PBS counterparts. Although some $PO_3^-$ is present within each spot, it is more likely that it is a contaminant from the microarray printing procedure. This is because the amount of $PO_3^-$ on the maleimide surface background (which is present before printing) is much lower. Some images have slightly higher distributions of $PO_3^-$ over a larger area such as 200 mM water spot unrinsed, while other images such as '0.1mM water spot unrinsed', contain $PO_3^-$ at a higher intensity closer to the image saturation intensity but the area where this intensity of $PO_3^-$ is found is much smaller. Rinsing the slide removes the $PO_3^-$ from the spot edges. We also see a decrease in the intensity of $PO_3^-$ in the spot centres such as in 2mM and 0.2mM water spots unrinsed.

## 5.4 Model of a PBS Spot Unrinsed

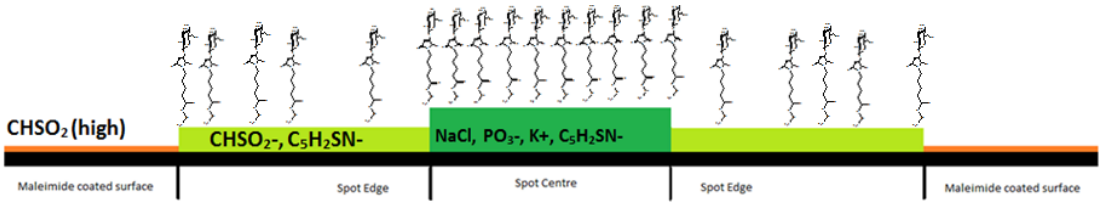


Figure 29 – Model of the 200 mM β-D-thioglucose PBS pre rinsed spot surface ion distribution showing the ions present in the different areas of the spots. Note that the saccharides shown are not on top of the contaminants.

In the schematic presentation of the spot chemistry in Figure 29, the entire slide which was previously maleimide functionalised is represented by the orange sections as the spaces between each spot in Figure 29. The light green section is the outer spot edge where the distance from the top surface to the amine coated surface is less than 2 nm which is the maximum depth ToF-SIMS can detect secondary ions from. $C_5H_2SN^-$, the ion which represents the β-D-thioglucose/maleimide surface interaction is more present at a higher intensity at the spot centre than at the spot edge.

This is an illustration of the β-D-thioglucose within a PBS spot's cross section on the slide. ToF-SIMS only detects the secondary ions from the top 2 nm of the surface. Certain ions such as $C_2H_2N^-$ below in Figure 30 are attributed to the amine or maleimide layer and are not detected at the spot centre which means the spot centre layers are thicker than 2 nm. This does not affect the spot edge which means its thickness is less than 2 nm.

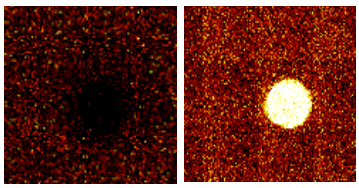

Figure 30 – Image showing the distribution of $Si^-$ in a unrinsed PBS spot(left) compared to an unrinsed $K^+$ ion distribution image (right) in 200 mM β-D-thioglucose spots.

The entire slide was previously maleimide functionalised and the orange sections above are the spaces between each spot. The light green section is the outer spot edge where the distance from the top surface to the amine coated surface is less than 2 nm which is the maximum depth ToF-SIMS can detect secondary ions from. This maximum detection depth is shown in Figure 30 where $Si^-$ is undetected at the spot centre because the amount of material (PBS components like $K^+$ and sugar compounds) forms a layer that is thicker than 2 nm.

## 5.5 Model of a PBS Spot Rinsed

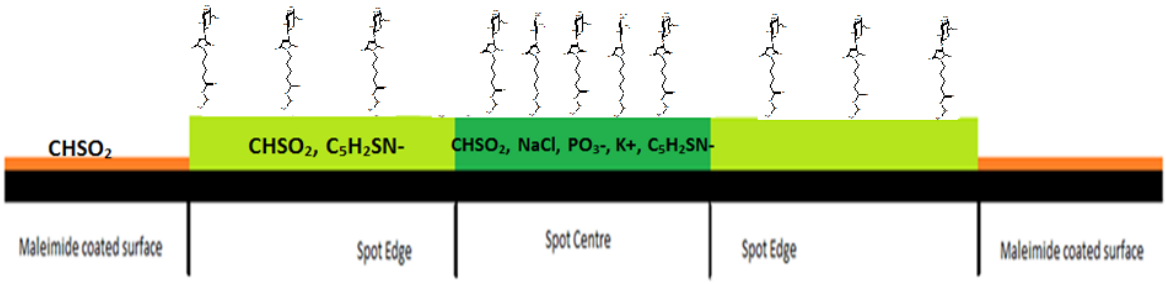


Figure 31 – Model of the 200 mM β-D-thioglucose PBS post rinse spot surface ion distribution showing the ions present at each region. Note that the saccharides shown are not on top of the contaminants.

Rinsing the spots reduces the thickness of the spot centre and removes material from the entire surface of the spot as shown in Figure 31. These substances include PBS salts and degraded β-D-thioglucose-maleimide compounds which are washed away.

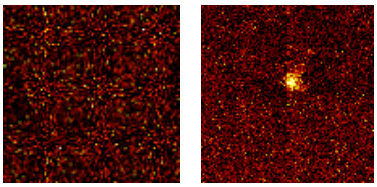

Figure 32 – Image showing the distribution of $C_2H_2N^-$ in a rinsed PBS spot(left) and $K^+$ ion distribution in a rinsed PBS spot (right) in 200 mM β-D-thioglucose spots.

In Figure 32, $C_2H_2N^-$ now has a uniform distribution on the surface including the spot centre which means rinsing removed some of the material at the spot centre. Therefore the entire spot must be below 2 nm in thickness post rinsing.

### 5.6 Model of a Water Spot Unrinsed

Below in Figure 33 is a proposed illustration of the cross section of a β-D-thioglucose in water spot. The main difference in both unrinsed spots (PBS and water) is that the spot edge is thicker in the water dissolved spot than in the PBS dissolved spot.

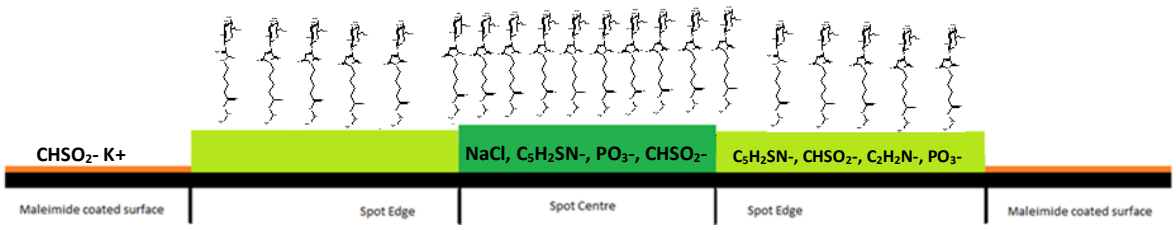


Figure 33 – Model of the 200 mM β-D-thioglucose Water pre rinse spot surface ion distribution showing the ions present at each region. Note that the saccharides shown are not on top of the contaminants.

Evidence of this is the decrease in the intensity of $K^+$ ions in the spot edge when compared to the maleimide surface outside the spot.

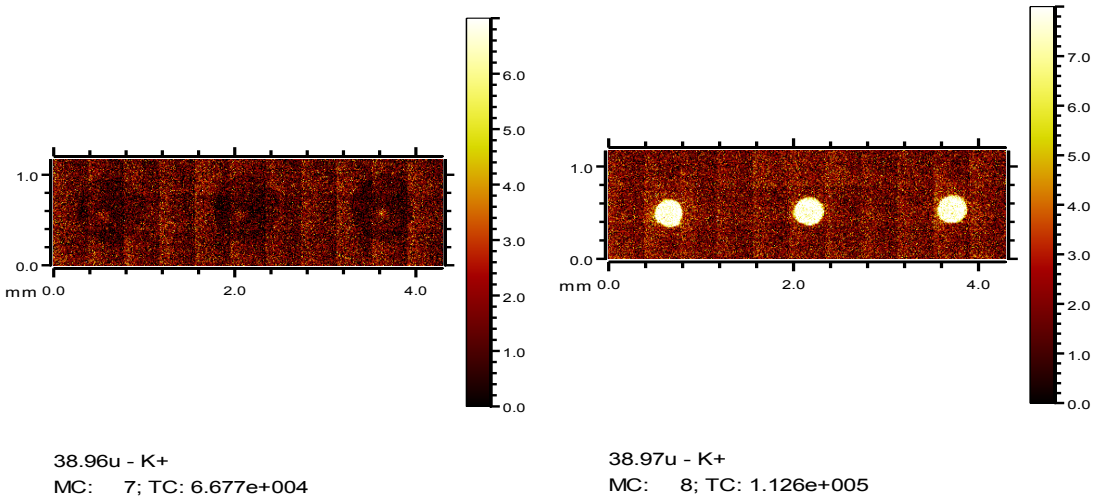


Figure 34 – SIMS images of $K^+$ ions in 200 mM β-D-thioglucose water spots (left) and 200 mM β-D-thioglucose PBS spots (right).

Because the water spot (left) had no PBS, the only source of potassium came from the maleimide slide where it has a uniform distribution. The spot edge has a lower intensity than the maleimide surface in Figure 34, which means the spot edge's thickness is higher in the water spots

than in the PBS spots. We can still detect some $K^+$ ions in the spot edge which means the thickness is still below 2 nm. There is a slight increase in the potassium intensity at the very centre of these spots which is more likely to be from some minor contamination and that $K^+$ is greatly affected by the matrix effect increasing its intensity beyond its true representation of the amount present. Scurr et al stated that PBS may inhibit saccharide interactions with the maleimide surface[5]. This is why they believe saccharides such as galactose(β1-4)glucose did not react with the spot centre because none was found in the region of the spot where the PBS components precipitated out the most which was the centre. Due to the decrease in the intensity of $K^+$ ions at the edge of the water spots it is very likely that the water spots are thicker because there is no PBS to inhibit β-D-thioglucose reacting with the maleimide surface. We do not see a decrease in $K^+$ in the same spot edge region of PBS spots because less saccharide material is present at those spot edges which may be due to some form of inhibitory interaction with some or all of the PBS components. However further research is required to confirm this.

## 5.7 Model of a Water Spot Rinsed

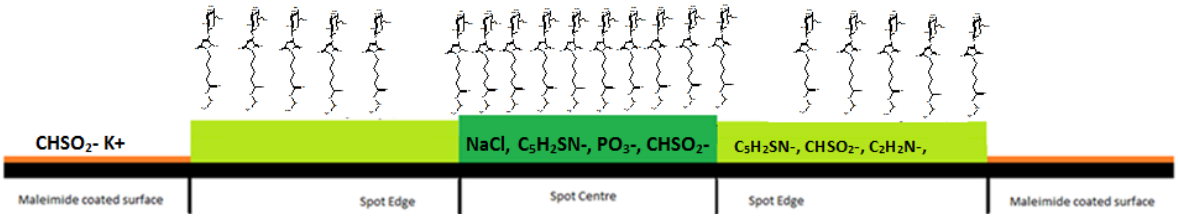


Figure 36 – Model of the 200 mM β-D-thioglucose Water post rinse spot surface ion distribution showing the ions present at each region. Note that the saccharides shown are not on top of the contaminants.

Rinsing the 200 mM Water spot removes the $K^+$ contamination at the spot centre. There is still a decrease in the $K^+$ ion intensity within the spot than on the maleimide surface background which is shown in Figure 36 below.

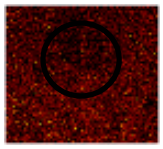

Figure 36 – Image showing the distribution of $K^+$ in a rinsed Water spot. The black circle highlights the loss of $K^+$ post rinsing when compared to the left image in Figure 41.

After rinsing there is still a difference in intensity in the spot when compared to the maleimide surface in the background. This difference shows that rinsing does not remove the β-D-thioglucose found at the spot edge. The intensity at the spot centre has decreased to match spot edge which means the material there has washed off sufficiently enough so that the depth of the spot centre is equal to the spot edge.

### 5.8 Results of the effect of β-D-thioglucose concentration on drying time

The graph below shows the relationship between β-D-thioglucose concentrations on drying time over various humidity's in PBS.

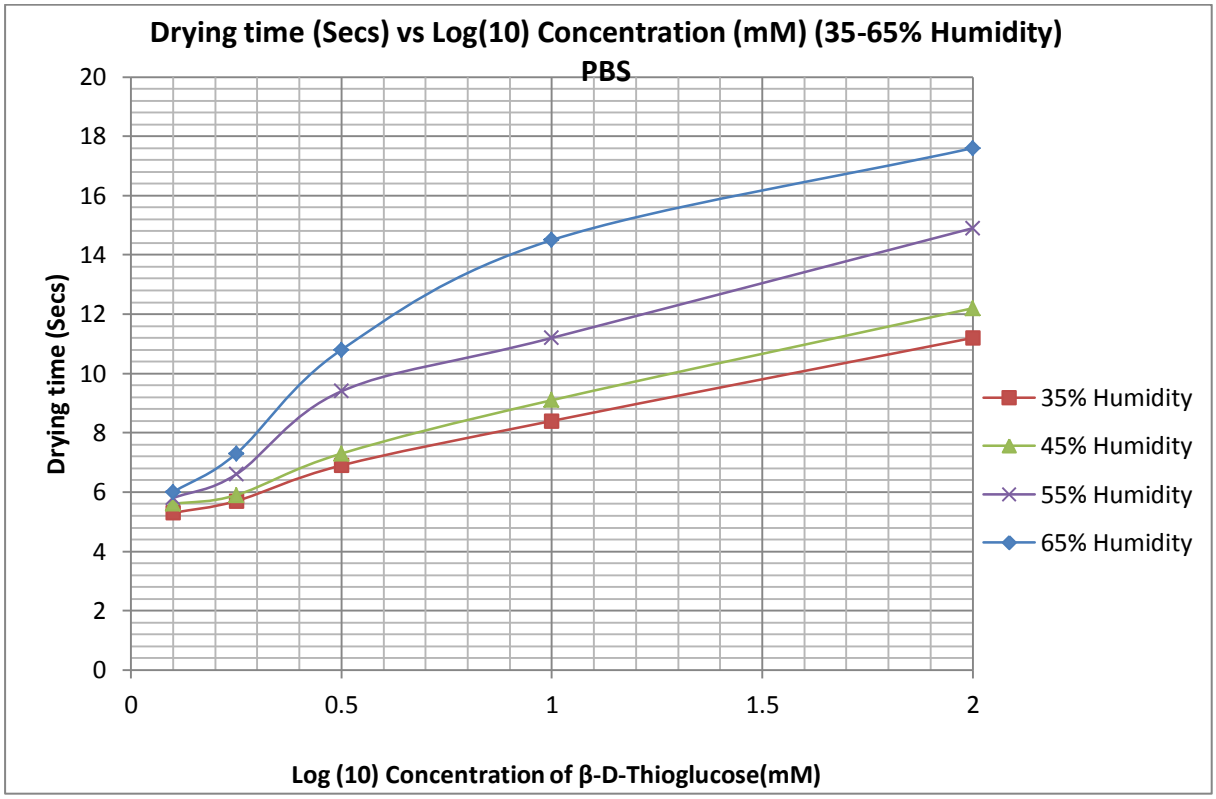


Figure 37 - Drying time (Secs) vs. Log(10) concentration (mM) (35-65% humidity) PBS.

As shown in Figure 37, increasing the concentration of β-D-thioglucose leads to an increase in the drying time of the spot. The rate of the increase in drying time is higher at higher humidity % like 55-65%. Initially the drying time is nearly equal at all humidity's when the concentration is at its lowest (Log (10) of 0.1mM). As the concentration of β-D-thioglucose increases we see a gradual difference in drying time occurring over different humidity's. This is where humidity has a greater effect than concentration. Once we reach a concentration of Log (10) of 0.7mM, the graph lines

become more parallel which suggests that humidity no longer strongly correlates with concentration. Although higher % humidity leads to slower drying times this is less and less dependent on concentration beyond Log (10) 0.7mM. Figure 45 shows us a graph from the same data but without any PBS:

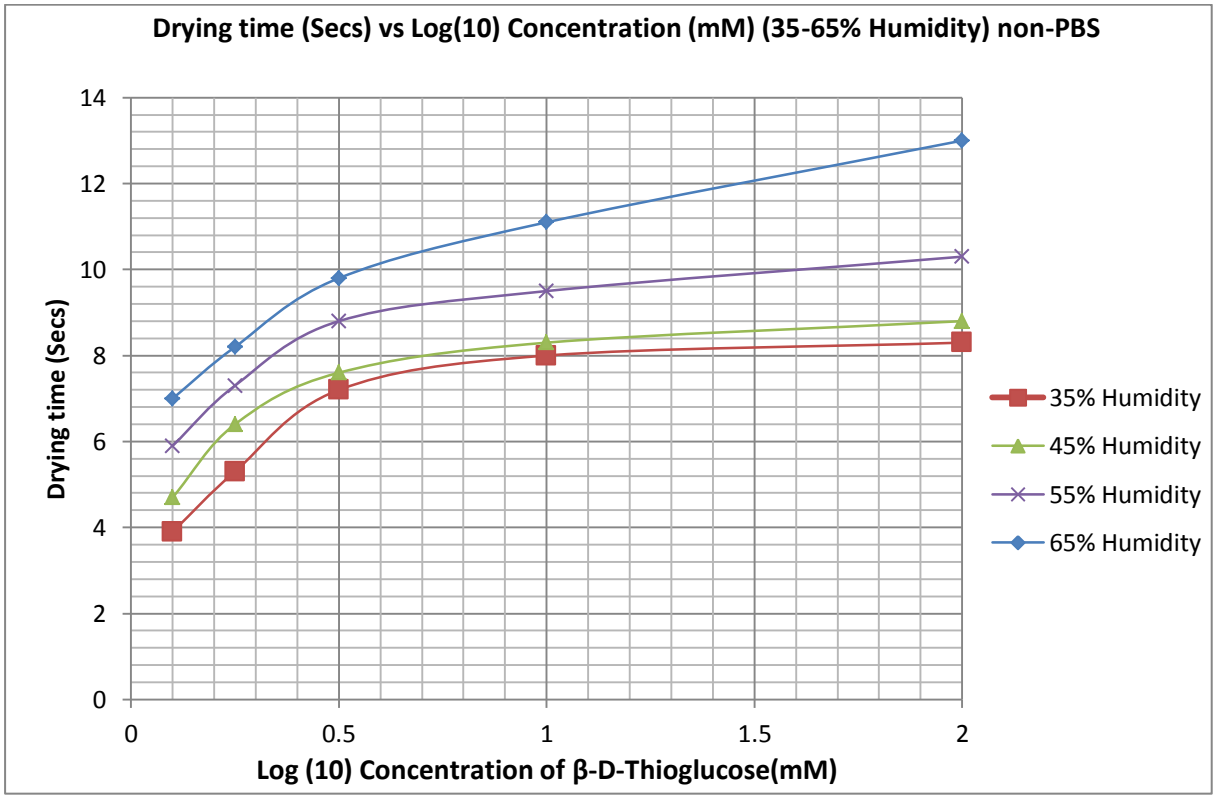


Figure 38 - Drying time (Secs) vs. Log(10) concentration (mM) (35-65% humidity) non-PBS

The main difference between both previous graphs (Figures 37 and 38) is that when PBS is not used the relationship between concentration and drying time is largely based on the effect of humidity. As we would expect the higher the humidity the higher the drying time. Just like in Figure 37 where the graph lines became parallel at Log (10) 0.7mM we also see parallel lines in terms of the

drying time in Figure 38. This trend occurs at a lower concentration of Log (10) 0.1mM. It is possible that at even lower concentrations below Log (10) 0.1mM we would see the same effects. Therefore when PBS is not used the concentration of β-D-thioglucose does not affect the drying time at any % humidity. This trend stops beyond Log (10) 1mM where we see a divergence of drying time at different humidities. As the concentration of β-D-thioglucose increases after Log (10) 1mM the drying time also increases. When the humidity is higher ($55\%^{+}$) β-D-thioglucose has an increased effect on drying time. Higher concentrations of β-D-thioglucose solutions are more viscous. The rate of solvent flow to the surface is reduced in more viscous solutions which increase the drying time. In more humid conditions the solvent molecules that eventually reach the surface to evaporate, also evaporate at a lower rate. These two factors (increased viscosity from an increased concentration in β-D-thioglucose and a more humid atmosphere) lead to higher drying times.

PBS like many dissolved solutes in water decreases the vapour pressure of water which decreases the rate of evaporation. The presence of PBS and β-D-thioglucose decreases the vapour pressure more than just with a solution of β-D-thioglucose. This is why the drying times are higher at the same concentrations of β-D-thioglucose when you compare the PBS and non-PBS containing graph points. For example: At 55% humidity in both Figures 37 and 38. The drying time in higher at a concentration of Log (10) 1mM when PBS is used (Figure 37, 11.2 seconds) than when PBS is excluded (Figure 38 9.5 seconds).

# 6. Future Work

One potential way of continuing this project would be to synthesise thiolated sugars due to the lack of commercially available ones. A particular thiolated sugar called 1-thiol-β-D-lactose can be synthesized using the following reaction scheme in Figure 39.

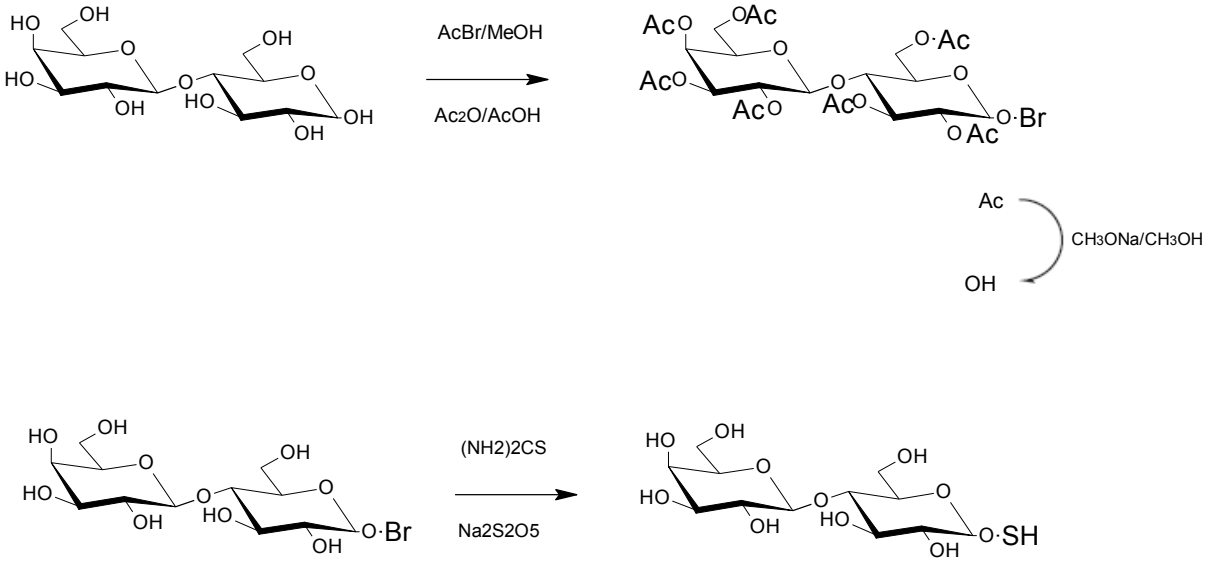


Figure 39 – Reaction scheme of 1-thiol-β-D-lactose synthesis[36].

This thiolated sugar will not be in a salt form and will provide a clearer insight into the effects of PBS on spot characteristics. A repeat of the previous work should be carried out on a smaller scale (amine coated slide>> maleimide coated slide>>carbohydrate microarray) where controls will be used to provide a better understanding on how each step affects the overall spot formation on microarrays. Such controls include the analysis of every reagent used as well as blank controls of just PBS and water as comparative data. This will ensure that the reagents used are not contaminant sources. Depth profiling should also be used to acquire data on how the surface chemistry changes from the spot surface to the amine layer.

# 7. Conclusions

The aim of this project is to produce glycan surfaces and characterise them in order to produce reliable readouts of the sample's surface and to discover the cause of unreliable readouts.

So far production of the glycan surfaces has occurred with β-D-thioglucose due to the presence of $C_5H_2SN^-$ detected during ToF-SIMS analysis which is an ion linked to β-D-thioglucose/maleimide covalent bonding. Glycan surfaces were not produced on spots where PBS was absent which means there is a strong possibility that PBS (or similar buffer) is required to facilitate the maleimide/thiol reaction. However the addition of PBS increases the spot drying time which may have provided enough time to allow a glycan surface to form.

The typical profile of the spots were a maleimide surface background (outside the spot), the thinner spot edge and the thicker spot centre. The spot edge was proved to be thinner when ions such as $CHSO_2^-$ were not present in the spot centre but were present uniformly in the spot edge and maleimide surface. ToF-SIMS cannot detect secondary ions below the top 2 nm showing that the spot centre pre rinse is higher than 2 nm. The chemistries differ between these three regions where the spot centre contains a higher amount of salt ions such as $Na^+$ with much lower amounts in the spot edges and far less outside the spot. Rinsing removes some of the material at the spot centre which means their presence is due to deposition during printing/drying and not due to covalent bonding. Some

thiolated sugars including β-D-thioglucose can form covalent bonds with the maleimide surface at the spot centres as well as the spot edge while other thiolated sugars form a distribution ring around the edge of the spot and not in the spot centre[5]. Finding out why some sugars behave this way is recommended when trying to produce reliable readouts of glycan surfaces.

The relationship between spot volume vs. drying time and sugar concentration vs. drying time at different humidities has also been investigated with the aim of seeing how the presence or absence of PBS affects these relationships. PBS has been found to increase the drying time of the drops by decreasing the vapour pressure and therefore the evaporation rate.

Given more time, the next steps in continuing this research would be to carry out production of more glycan surfaces with synthesized thiolated sugars and discovering the reasons why some spots are not reliably produced. This work would then continue on to produce surface glycan ligand models of cells.

**Acknowledgements**

**Moamen Hammad** – My LBSA buddy which provided me with excellent answers to many questions I had throughout the year.

**David Scurr** – He helped me carry out all of the ToF-SIMS analysis throughout the year and taught me how to operate the ION-TOF software needed to process the vast information acquired. He also provided useful advice on SIMS analysis.

**Andrew Hook** – He helped me carry out the entire microarray printing throughout the year and also taught me how to pre-treat the glass slides for maleimide functionalization.

**Fabio Simones** - Fabio has been a great help in integrating me into the LBSA department.

**Morgan Alexander** - My principal supervisor who has been a great person to work under and got me involved with this fascinating research in the first place. He has provided me with valuable insight into the inner workings of the scientific community.

**Training Received**

New Research Workers Health and Safety Training - Induction phase

Workspace – Sciquest Training – Hammad Moaman, Sciquest Training course

Lab Safety for Working in C24/D38 Lab – Paul Cooling

Lab Safety for Working in B15 Lab – Sebastian Spain

AFM Training 1 - Dr Xinyong Chen

AFM Training 2 - Dr Xinyong Chen

ToF-SIMS Training – Dr David Scurr

Using Microarray Printers – Dr Andrew Hook

# References


1. Weishaupt, M., S. Eller, and P.H. Seeberger, *Chapter Twenty-Two - Solid Phase Synthesis of Oligosaccharides*, in *Methods in Enzymology*, F. Minoru, Editor 2010, Academic Press. p. 463-484.
2. Ma, Z. and F. Zaera, *Organic chemistry on solid surfaces.* Surface Science Reports, 2006. **61**(5): p. 229-281.
3. Watcharatanyatip, K., et al., *Multispecies detection of antibodies to influenza A viruses by a double-antigen sandwich ELISA.* Journal of Virological Methods, 2010. **163**(2): p. 238-243.
4. Wu, Z.Z., Y.P. Zhao, and W.S. Kisaalita, *A packed Cytodex microbead array for three-dimensional cell-based biosensing.* Biosensors and Bioelectronics, 2006. **22**(5): p. 685-693.
5. David J. Scurr, T.H., Matthias A. Oberli, Daniel B. Werz, Lenz Kroeck, and P.H.S. Simone Bufali, Alexander G. Shard, and Morgan R. Alexander, *Surface Characterization of Carbohydrate Microarrays.* Langmuir, 2010. **26**(22): p. 17143–17155.
6. Vlachopoulou, M.-E., et al., *Protein arrays on high-surface-area plasma-nanotextured poly(dimethylsiloxane)-coated glass slides.* Colloids and Surfaces B: Biointerfaces, 2011. **83**(2): p. 270-276.
7. Sonya M. Khersonsky, C.M.H., Mary-anne F. Garcia and Young-Tae and Chang, *Recent Advances in Glycomics and Glycogenetics.* Current Topics in Medicinal Chemistry, 2003. **3**: p. 617-643.
8. Hashide, R., et al., *Insulin-containing layer-by-layer films deposited on poly(lactic acid) microbeads for pH-controlled release of insulin.* Colloids and Surfaces B: Biointerfaces, 2012. **89**(0): p. 242-247.
9. Zem, G.C., et al., *Microbead analysis of cell binding to immobilized lectin: an alternative to microarrays in the development of carbohydrate drugs and diagnostic tests.* Acta Histochemica, 2006. **108**(4): p. 311-317.
10. Tanifum, C.T., J. Zhang, and C.-W.T. Chang, *Combination of solid phase and solution phase synthesis of oligosaccharides using sonication.* Tetrahedron Letters, 2010. **51**(33): p. 4323-4327.
11. Weijers, C.A.G.M., M.C.R. Franssen, and G.M. Visser, *Glycosyltransferase-catalyzed synthesis of bioactive oligosaccharides.* Biotechnology Advances, 2008. **26**(5): p. 436-456.
12. Jang-Lee, J., et al., *Glycomic Profiling of Cells and Tissues by Mass Spectrometry: Fingerprinting and Sequencing Methodologies*, in *Methods in Enzymology*, F. Minoru, Editor 2006, Academic Press. p. 59-86.
13. Fais, M., et al., *Lectin and carbohydrate microarrays: New high-throughput methods for glycoprotein, carbohydrate-binding protein and carbohydrate-active enzyme analysis.* Journal of Cereal Science, 2009. **50**(3): p. 306-311.
14. Zhou, X. and J. Zhou, *Oligosaccharide microarrays fabricated on aminooxyacetyl functionalized glass surface for characterization of carbohydrate–protein interaction.* Biosensors and Bioelectronics, 2006. **21**(8): p. 1451-1458.
15. Disney, M.D. and P.H. Seeberger, *Carbohydrate arrays as tools for the glycomics revolution.* Drug Discovery Today: TARGETS, 2004. **3**(4): p. 151-158.
16. Lee, M.-r., S. Park, and I. Shin, *Protein microarrays to study carbohydrate-recognition events.* Bioorganic & Medicinal Chemistry Letters, 2006. **16**(19): p. 5132-5135.
17. Song, E.-H. and N.L.B. Pohl, *Carbohydrate arrays: recent developments in fabrication and detection methods with applications.* Current Opinion in Chemical Biology, 2009. **13**(5-6): p. 626-632.
18. Hart, G.W. and R.J. Copeland, *Glycomics Hits the Big Time.* Cell, 2010. **143**(5): p. 672-676.

19. Khoury, G.A., R.C. Baliban, and C.A. Floudas, *Proteome-wide post-translational modification statistics: frequency analysis and curation of the swiss-prot database.* Sci. Rep., 2011. **1**.
20. Ishizuka, Y., et al., *Application of ultra-high magnetic field for saccharide molecules: 1H NMR spectra of 6-O-α-d-glucopyranosyl-cyclomaltoheptaose and -cyclomaltohexaose.* Carbohydrate Research, 2005. **340**(7): p. 1343-1350.
21. Awatani, T., et al., *Morphology of water transport channels and hydrophobic clusters in Nafion from high spatial resolution AFM-IR spectroscopy and imaging.* Electrochemistry Communications, 2013. **30**(0): p. 5-8.
22. Staicopolus, D.N., *The computation of surface tension and of contact angle by the sessile-drop method.* Journal of Colloid Science, 1962. **17**(5): p. 439-447.
23. Vickerman, J.C. and I.S. Gilmore, in *Surface Analysis – The Principal Techniques*2009, John Wiley & Sons, Ltd.
24. Stephan, T., *TOF-SIMS in cosmochemistry.* Planetary and Space Science, 2001. **49**(9): p. 859-906.
25. Hook, D.J., et al., *Quantitative and high mass ToF-SIMS studies of siloxane segregation in hydrogel polymers using cryogenic sample handling techniques.* Applied Surface Science, 2006. **252**(19): p. 6679-6682.
26. Trevisiol, E., et al., *Dendrislides, dendrichips: a simple chemical functionalization of glass slides with phosphorus dendrimers as an effective means for the preparation of biochips.* New Journal of Chemistry, 2003. **27**(12): p. 1713-1719.
27. Barnes, T.J., I.M. Kempson, and C.A. Prestidge, *Surface analysis for compositional, chemical and structural imaging in pharmaceutics with mass spectrometry: A ToF-SIMS perspective.* International Journal of Pharmaceutics, 2011. **417**(1–2): p. 61-69.
28. Lima, M.M. and R. Monteiro, *Characterisation and thermal behaviour of a borosilicate glass.* Thermochimica Acta, 2001. **373**(1): p. 69-74.
29. Hulen, C. and F. Le Goffic, *Analysis of peptide uptake in Pseudomonas aeruginosa: A fluorescamine labeling procedure.* FEMS Microbiology Letters, 1987. **40**(1): p. 103-109.
30. Sandu, I. and C.T. Fleaca, *The influence of gravity on the distribution of the deposit formed onto a substrate by sessile, hanging, and sandwiched hanging drop evaporation.* Journal of Colloid and Interface Science, 2011. **358**(2): p. 621-625.
31. Sritapunya, T., et al., *Wetting of polymer surfaces by aqueous surfactant solutions.* Colloids and Surfaces A: Physicochemical and Engineering Aspects, 2012. **409**(0): p. 30-41.
32. Gelhausen, M., et al., *Lectin recognition of liposomes containing neoglycolipids. Influence of their lipidic anchor and spacer length.* Colloids and Surfaces B: Biointerfaces, 1998. **10**(6): p. 395-404.
33. Sanganwar, G.P. and R.B. Gupta, *Nano-mixing of dipyridamole drug and excipient nanoparticles by sonication in liquid CO2.* Powder Technology, 2009. **196**(1): p. 36-49.
34. Saint-Hilaire, D., K.Z. Ismail, and U. Jans, *Reaction of tris(2-chloroethyl)phosphate with reduced sulfur species.* Chemosphere, 2011. **83**(7): p. 941-947.
35. Yang, Y., et al., *Characterization of multivalent lactose quantum dots and its application in carbohydrate–protein interactions study and cell imaging.* Bioorganic & Medicinal Chemistry, 2010. **18**(14): p. 5234-5240.
36. Yang, Y., et al., *Characterization of multivalent lactose quantum dots and its application in carbohydrate–protein interactions study and cell imaging.* Bioorganic & Medicinal Chemistry, 2010. **18**(14): p. 5234-5240.